

STUDYING THE DECAY OF $^{46}\text{TI}^*$: ENTRANCE CHANNEL AND/OR α -STRUCTURE EFFECTS?



Fabiana GRAMEGNA



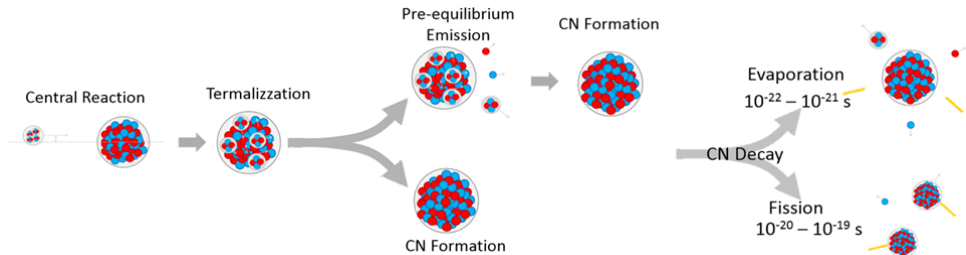
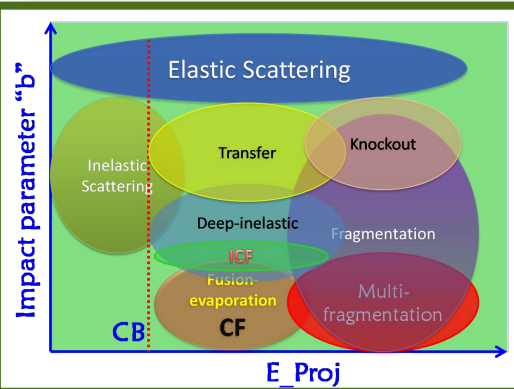
INFN - Laboratori Nazionali di Legnaro

OUTLINE

- Fusion reaction between light/medium nuclei: fast & thermal emission competition, structure effects, clustering
- The $^{46}\text{Ti}^*$ formed through different entrance channels
- Simulations, geometrical filters and data selections
- Experimental Results & comparison to model predictions
- Conclusions

Reaction Mechanisms

$$E_p > B_C \Rightarrow \sigma_{reaz} = \sum_{\ell} \sigma_{reaz} (\ell) = \frac{\pi}{k^2} \sum_0^{\infty} (2\ell + 1) T_{\ell}$$



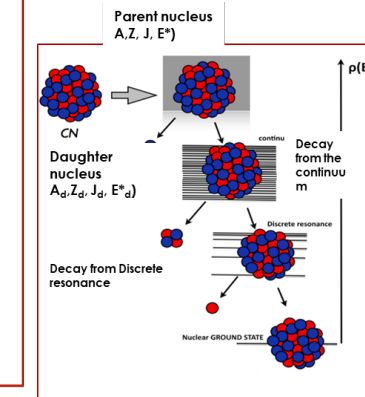
EXP: highly exclusive detection **NUCL-EX collaboration**

campaign:

- STATistical properties of LIGHT nuclei from Fus-Evap.
- ACLUST-ACLUST2: Study of the competition between fast and thermal emission from a hot source

GARFIELD+RCo @ LNL

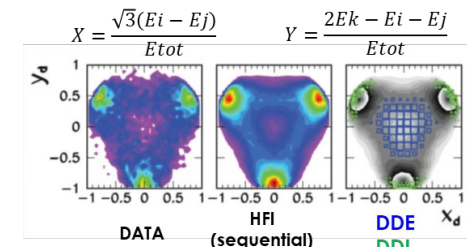
- ❖ low multiplicity events & high detection coverage
- ❖ high energy and angular resolution
- ❖ complete event Reconstruction
- ❖ global control on the decay mechanism



Hoyle State in $^{12}\text{C} + ^{12}\text{C}$ reaction

L. Morelli et al. J.Phys.G 43(2016) 045110

Energy DALITZ Plot



❑ **Hot light nuclei** ($E^* \sim 3$ A.MeV) → produced in **multi-fragmentation** in a wide range of N/Z → **TRACING BACK** → access to the **symmetry energy term** in the NEOS

➢ **Limiting Temperature**

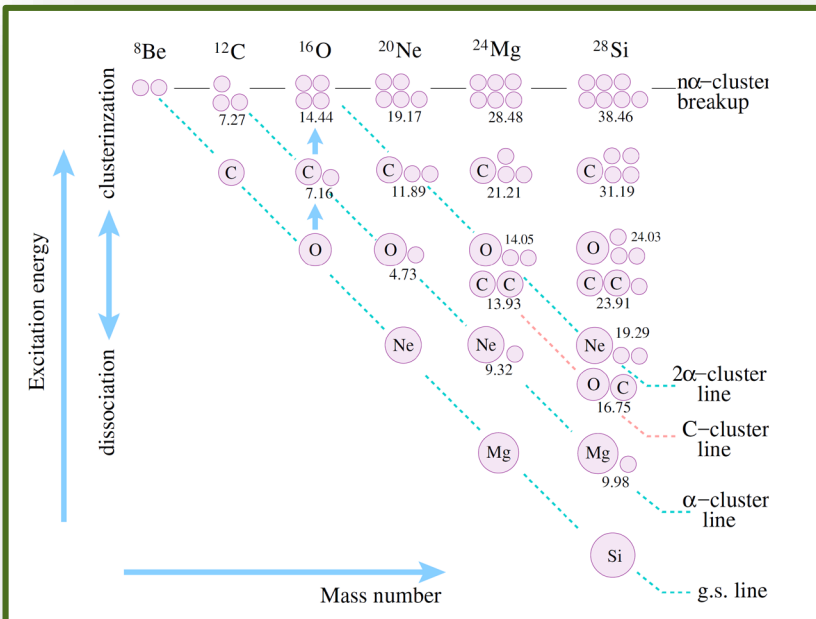
➢ only access to **level densities** above the **thresholds for particle decay** via evaporation reactions (**compound nucleus decay theory**) → decreasing of **NLD** as a function of increasing **N-Z**

➢ mainly **inclusive experiments** → lack of complete studies on the evaporation from light nuclei especially in the mass region **A~20**

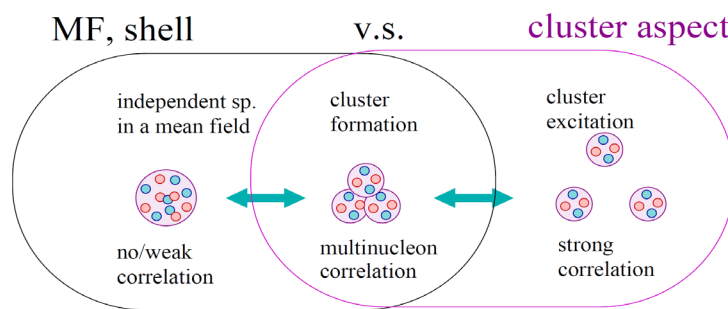
➢ Some **excited states** of different nuclei in this mass region are known to present **pronounced clustered structures**

❑ **Medium light nuclei** → studying the competition between **fast** and **thermal emission** from a **hot source** → **pre-equilibrium processes** → **cluster emission** → link to **structure effects or dynamical formation?**

Studying Nuclear clustering



Y. Kanada-En'yo, International School of Physics "Enrico Fermi", course 201
(Nuclear Physics with Stable and Radioactive Beams), 14-19 July 2017



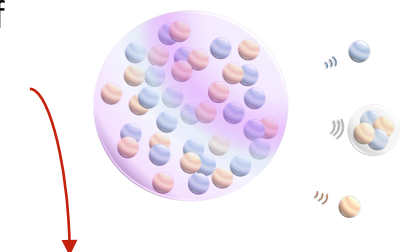
Light Nuclei

Coexistence of cluster and mean-fields aspects:
connection between cluster emission and nuclear structure.

Medium Mass Nuclei

Clustering effects on reaction dynamics can be **observed**. Are they due to **cluster pre-formation** either in the colliding partners or in the CN* or do they derive by a **dynamical formation**.

Analyzing the competition of
CF with **fast processes** →
Thermal vs pre-equilibrium
particles emission



Studying the competition between evaporation (surface) and fast (volume) emission of LCP.

- Y. Kanada-En'yo et al., Prog.Theo.Exp.Phys. 01A202 (2012).
- P.E. Hodgson, E. Běták, Phys. Rep. 374 (2003) 1-89.

The $^{46}\text{Ti}^*$ formed through different entrance channels

Entrance channel	$E_{\text{beam, lab}}$		θ_{grazing}	CN	η	σ_{fus}	E^*	Lcrit (Bass)	Lab. Vel.	E.R. Distrib. θ_{lab}
Beam + Target	MeV	MeV/u	deg			mb	MeV	hbar	cm/ns	deg
$^{16}\text{O} + ^{30}\text{Si}$	128	8	8,8	^{46}Ti	0,304	1070	98,4	37.3	1,37	0 – 30
$^{16}\text{O} + ^{30}\text{Si}$	111	7	10,1	^{46}Ti	0,304	1081	88,0	35.4	1,28	0 – 30
$^{18}\text{O} + ^{28}\text{Si}$	126	7	9,0	^{46}Ti	0,217	1110	98,5	37.7	1,44	0 – 28
$^{19}\text{F} + ^{27}\text{Al}$	133	7	8,9	^{46}Ti	0,174	1100	103,5	38.3	1,52	0 – 28

same beam velocity



same pre-equilibrium component

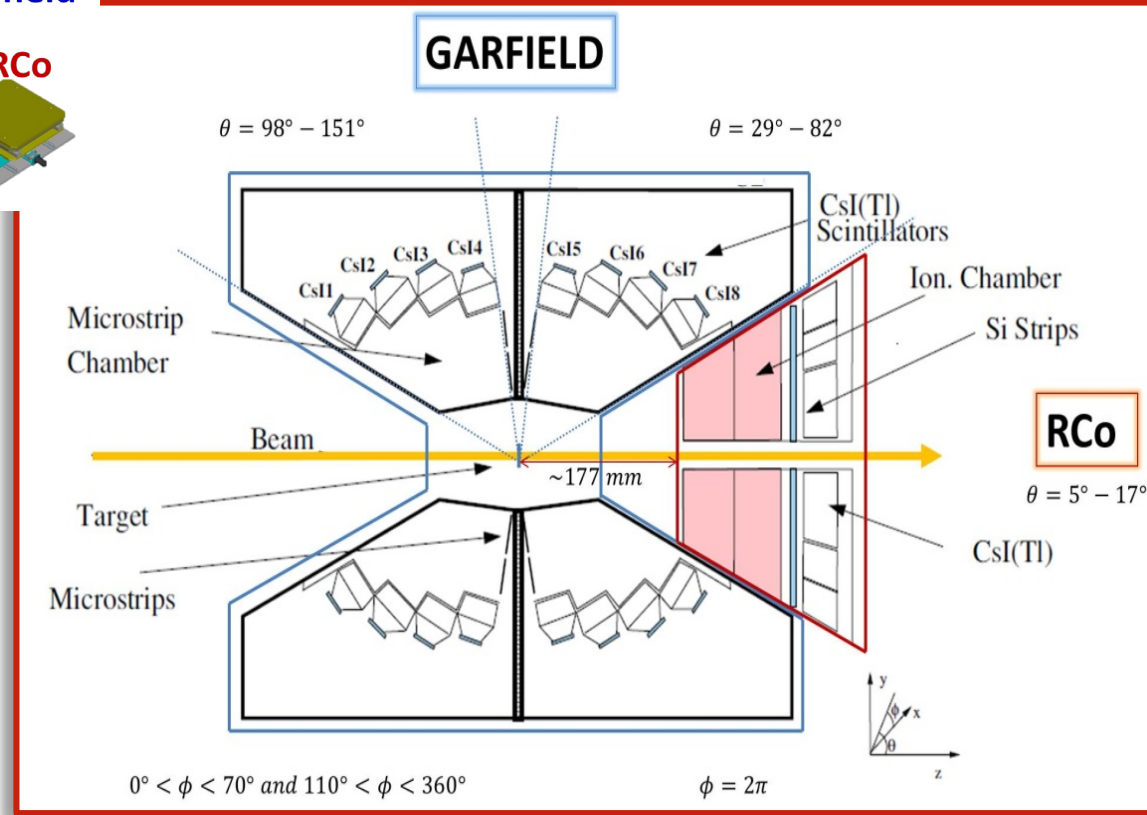
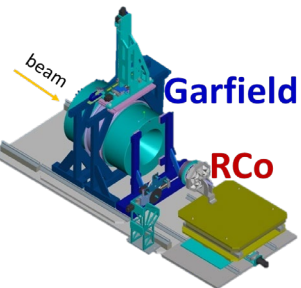
same CN Excitation Energy



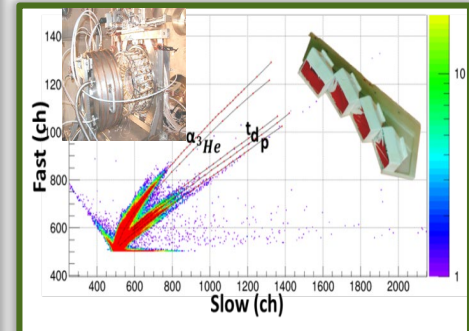
same statistical component

The Experimental Set-up

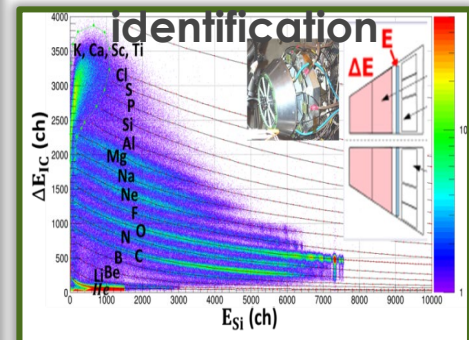
GARFIELD + RCo



LCP identification



RESIDUE identification



- F. Gramegna et al., Proc. of IEEE Nucl.Symp., 2004, Roma, Italy, 0-7803-8701-5/04/.
- M. Bruno et al. Eur. Phys. J. A (2013) 49: 128

**Selection of
CENTRAL EVENTS**



Evaporation Residue is detected in coincidence with Light Particles

Effects of Structure of Interacting Nuclei & Reaction Dynamics

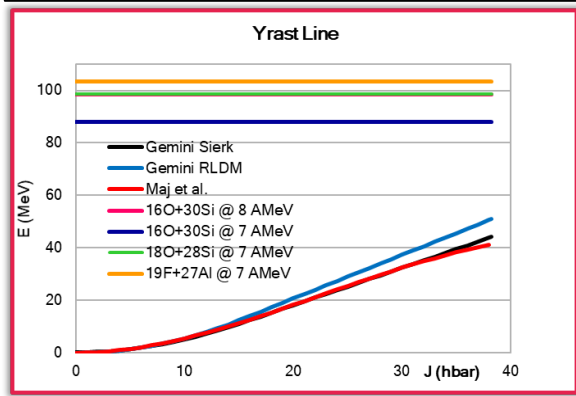
8 MeV/n $^{16}\text{O}+^{30}\text{Si}$
 7 MeV/n $^{16}\text{O}+^{30}\text{Si}$
 7 MeV/n $^{18}\text{O}+^{28}\text{Si}$
 7 MeV/n $^{19}\text{F}+^{27}\text{Al}$

$^{46}\text{Ti}^*$
DECAY

GEMINI++ (R. J. Charity, Phys Rev C82 (2010) 014610.)

Simulate the **decay of hot nuclei** formed in fusion/quasi-fusion reaction.

- **Standalone** → a good selection of central events can be performed; different code parameters can be set.



3. Level density

$$\rho_B(E_B^*) \propto 2\sqrt{aE_B^*}$$

$$a = \frac{A}{k_\infty - (k_\infty - k_0)\exp\left(-\frac{\kappa}{k_\infty - k_0} U\right)}$$

$$\kappa(A) = 0.000517\exp(0.0345A)$$

DEFORMED NUCLEUS

{M. Brekiesz et al., Nucl.Phys A 788 (2007) 224c-230c}

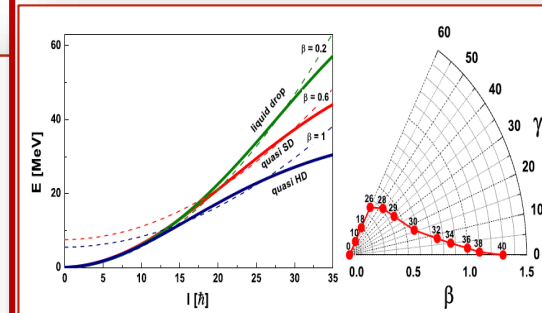
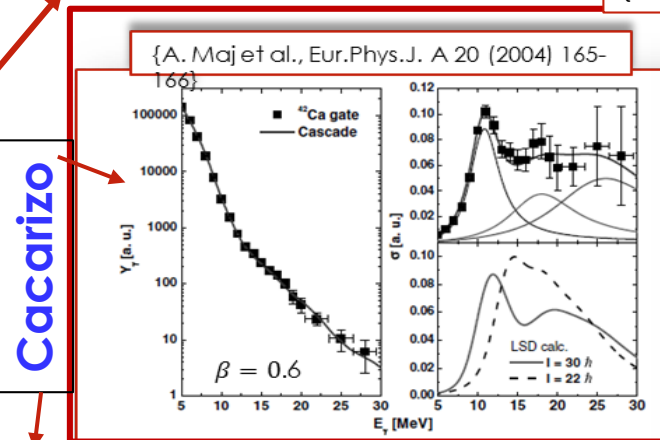


Figure 2. Left: the yrast lines used in the calculations (solid lines) and the rigid body yrast lines with different deformation parameters (dotted lines). Right: the evolution of the equilibrium shape of ^{46}Ti as a function of spin predicted by the LSD model.

β	δ_1	δ_2	Shape
0.2	<i>RLDM</i> parameters		
0.6	4.6×10^{-4}	1.0×10^{-7}	Quasi – SUPERDEFORMED
1.0	1.1×10^{-3}	1.0×10^{-7}	Quasi – HYPERDEFORMED

1. Macroscopic Rotational Energy

$$E_{Yrast}(J) = \begin{cases} E_{Sierk}(J) & \text{if } J < J^* \\ E_{Sierk}(J) + (J - J^*)E_{Sierk}(J^*) & \text{if } J > J^*, J^* = 0.319A \end{cases}$$

2. Transmission coefficients

$$T_l(\epsilon) = \frac{T_l^{R_0-\delta r}(\epsilon) + T_l^{R_0}(\epsilon) + T_l^{R_0+\delta r}(\epsilon)}{3}, \delta r = w\sqrt{T}$$

a) w=0.0 G00, b) w=1.0 G10, c) w=1.1 G11

Antisymmetrized Molecular Dynamics {A. Ono, Phys. Rev. C59, 853 (1999)}

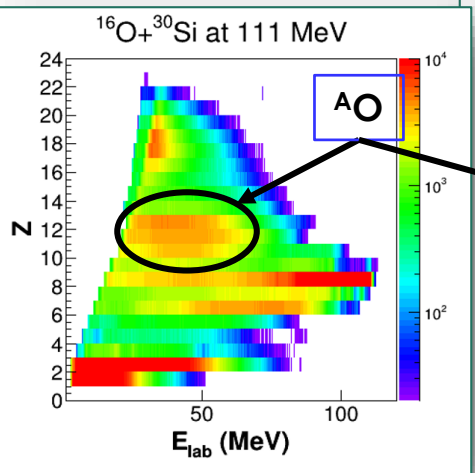
- describes the cluster structure of the interacting particles.
- takes into account the particle-particle correlations.

HIPSE {D. Lacroix, et al., Phys. Rev. C69, 054604 (2004)}

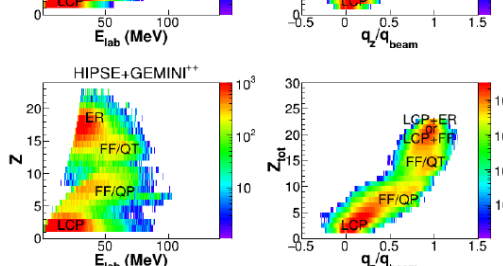
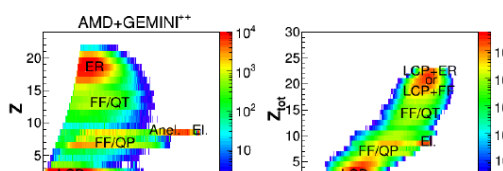
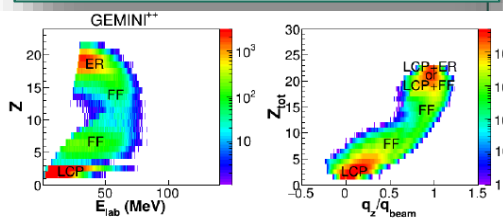
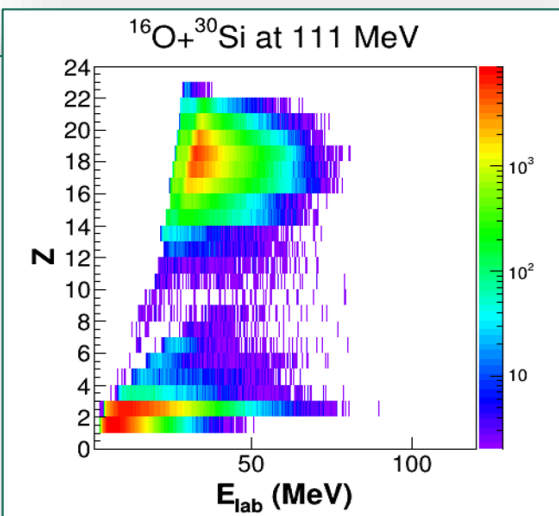
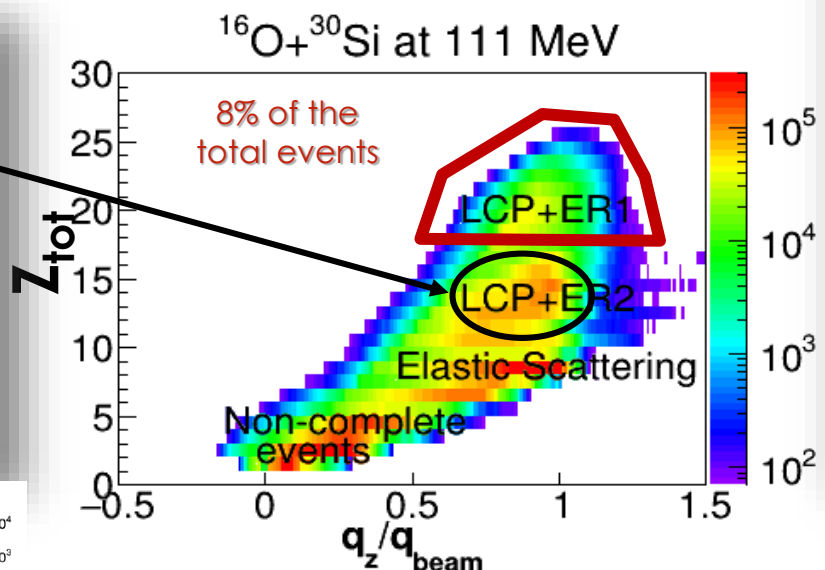
- describes nuclear collisions of heavy-ions in the intermediate energy range.
- Based on sudden approximation.

GEMINI++ as Afterburner (after a dynamical code) to produce **secondary particles distributions** from primary fragments → to be compared with exp data.

Z vs E_{lab}



Correlation between the **longitudinal momentum** and the **total detected charge**

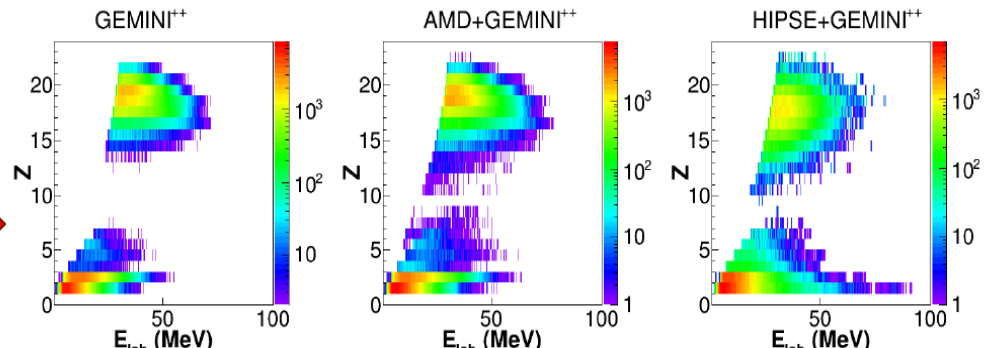


To cut **contamination events** we need to ask at least $Z_{tot} > 16 = O+O$

More restrictive: selecting almost **complete events**

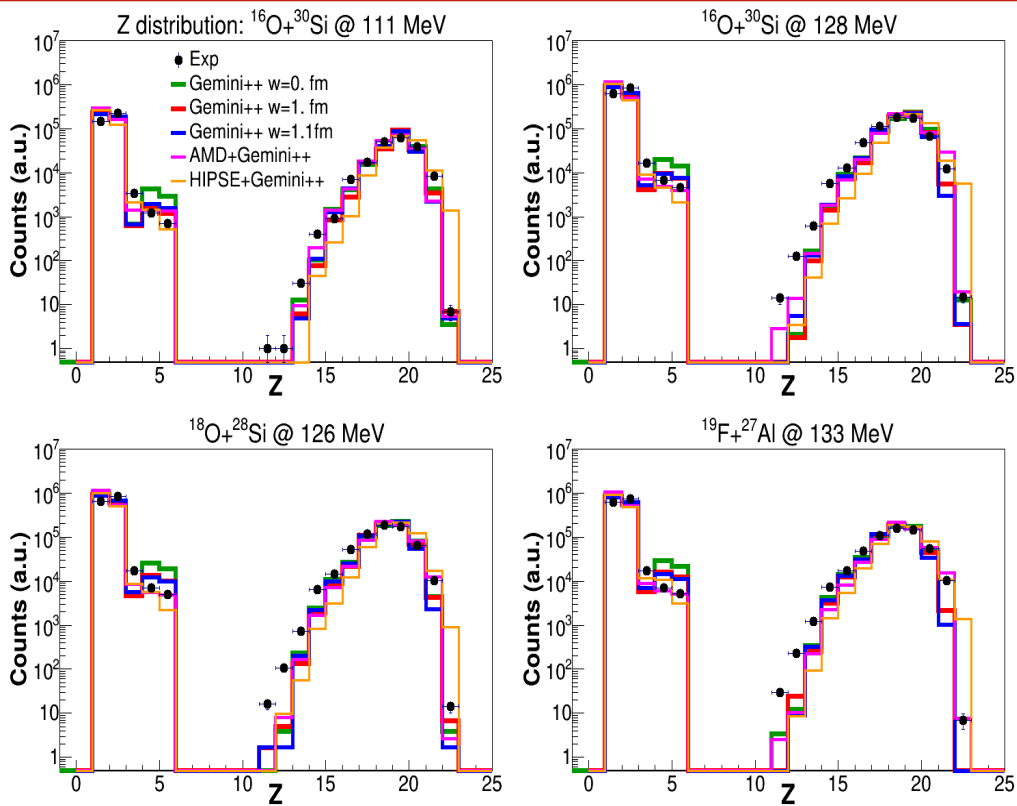
- $Z_{tot} > 18 (>82\%)$
- $q_z/q_{beam} < 1.2$

Same cuts on simulations !!!!!



Results: $Z_{\text{tot}} = Z_p + Z_t = 22$

Complete events - **Z-distribution**



● Exp

- Green: Gemini++ w=0. fm
- Red: Gemini++ w=1. fm
- Blue: Gemini++ w=1.1 fm
- Magenta: AMD+Gemini++
- Orange: HIPSE+Gemini++

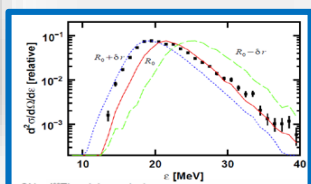
→ Unique barrier G00

→ Deformation 2:1 G10

→ Deformation 2.2:1 G11

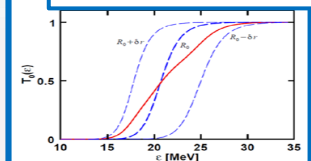
TOTAL CHARGE DETECTED
Only neutrons missing

$\frac{\# \text{Evts } Z_{\text{tot}}=22}{\# \text{Tot Evts}}$	$^{16}\text{O}+^{30}\text{Si}$ 111 MeV	$^{16}\text{O}+^{30}\text{Si}$ 128 MeV	$^{18}\text{O}+^{28}\text{Si}$ 126 MeV	$^{19}\text{F}+^{27}\text{Al}$ 133 MeV
Experimental	0.3%	0.3%	0.4%	0.6%
GEMINI++ w=0.0 fm	3.4%	3.6%	3.9%	3.9%
GEMINI++ w=1.0 fm	4.0%	4.1%	4.5%	4.3%
GEMINI++ w=1.1 fm	3.8%	3.9%	4.4%	4.3%
AMD+GEMINI++	2.5%	2.8%	3.4%	3.3%
HIPSE+GEMINI++	2.8%	2.9%	3.2%	2.7%



$$T_l(\epsilon) = \frac{T_l^{R_0-\delta r}(\epsilon) + T_l^{R_0}(\epsilon) + T_l^{R_0+\delta r}(\epsilon)}{3}, \delta r = w\sqrt{T}$$

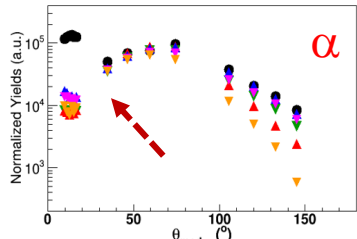
{R. J. Charity, Phys Rev C 82 (2010) 014610}



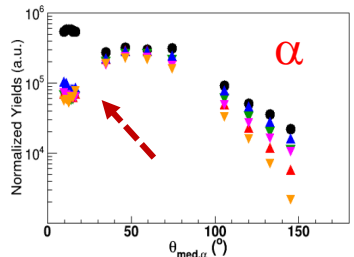
Results: $Z_{\text{tot}} = Z_p + Z_t = 22$

Ang. Distributions & Multiplicities

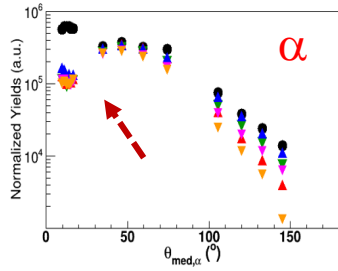
$^{16}\text{O} + ^{30}\text{Si}$ 111MeV



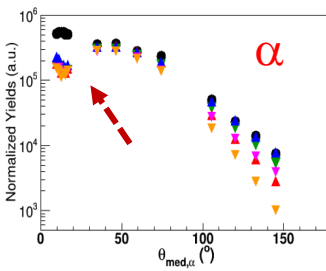
$^{16}\text{O} + ^{30}\text{Si}$ 128MeV



$^{18}\text{O} + ^{28}\text{Si}$ 126MeV

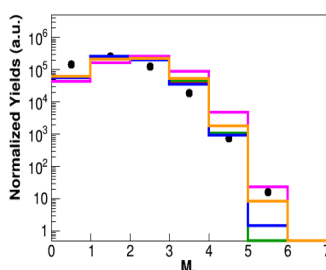
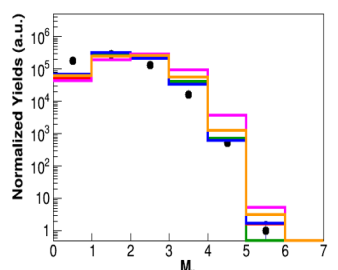
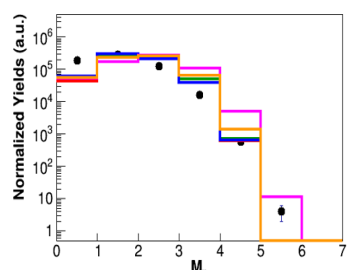
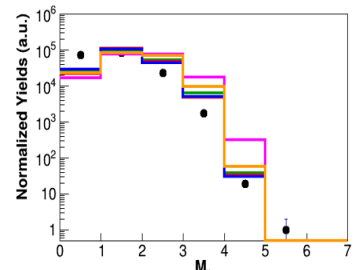
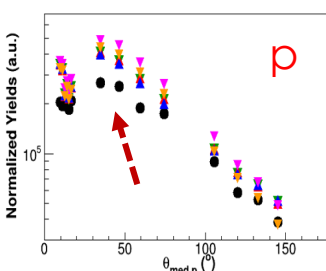
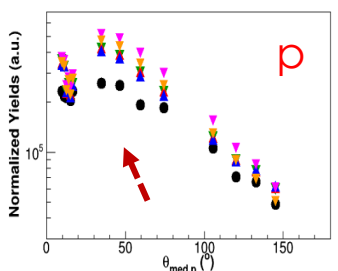
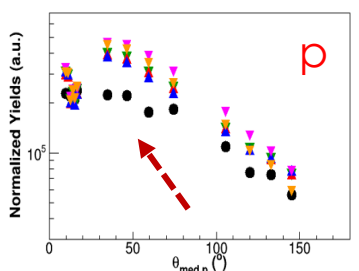
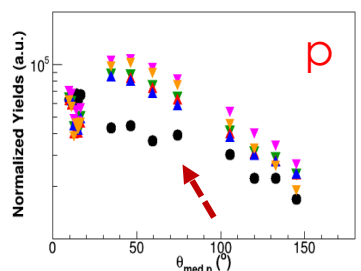
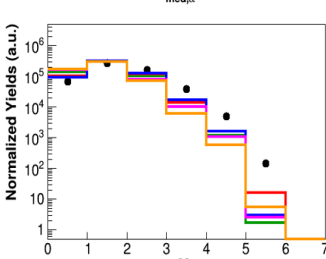
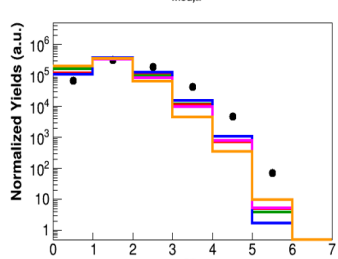
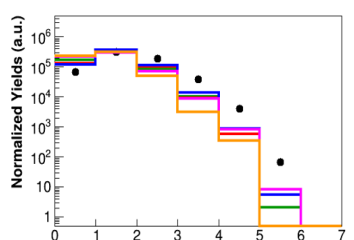
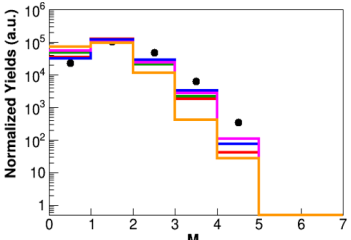


$^{19}\text{F} + ^{27}\text{Al}$ 133MeV



● Exp.
 ▼ GEMINI⁺⁺: w=0.0fm
 ▲ GEMINI⁺⁺: w=1.0fm
 △ GEMINI⁺⁺: w=1.1fm
 ■ AMD+GEMINI⁺⁺
 □ HIPSE+GEMINI⁺⁺

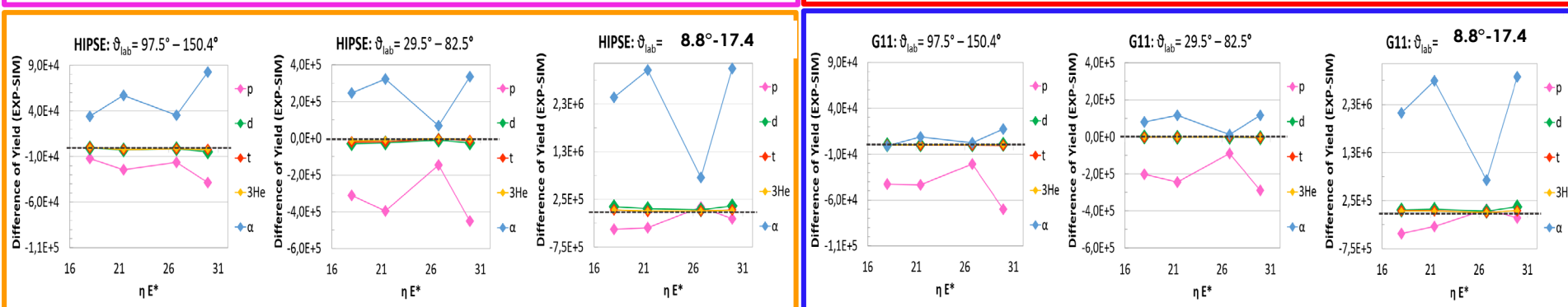
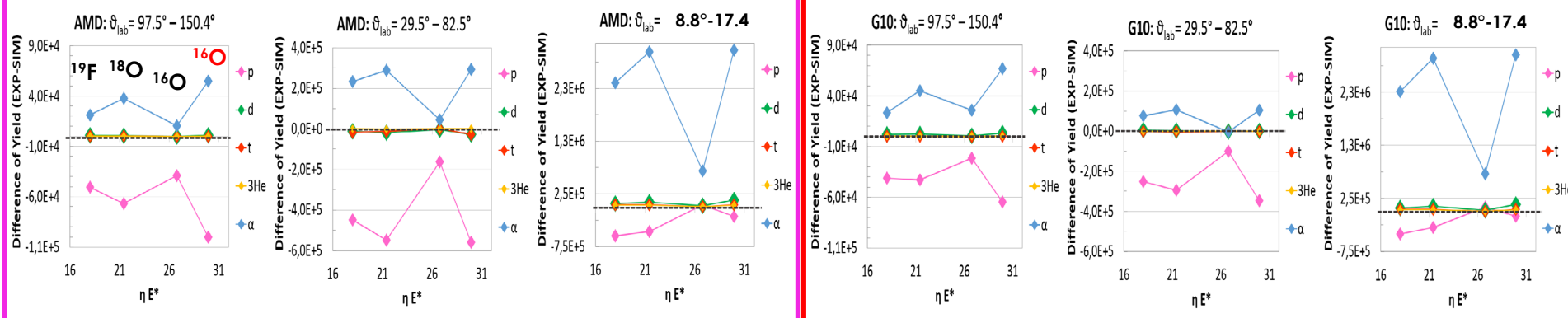
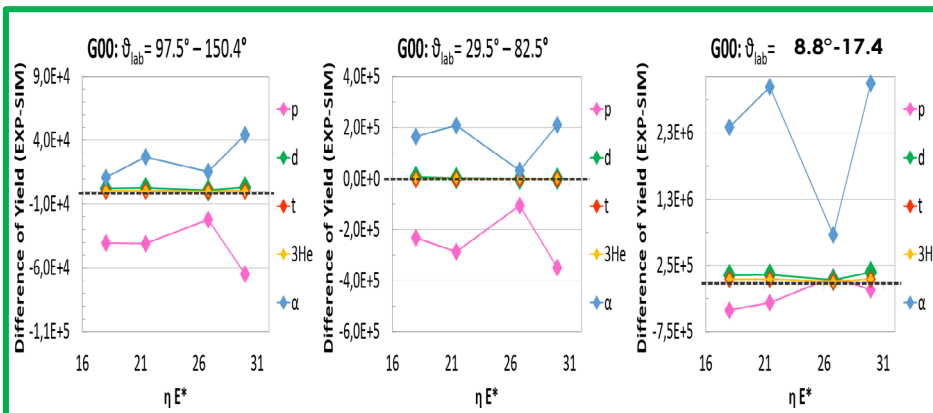
● Exp.
 — GEMINI⁺⁺: w=0.0fm
 — GEMINI⁺⁺: w=1.0fm
 — GEMINI⁺⁺: w=1.1fm
 ■ AMD+GEMINI⁺⁺
 — HIPSE+GEMINI⁺⁺



Results: $Z_{\text{tot}} = Z_p + Z_t = 22$

Ang. Distributions Differences

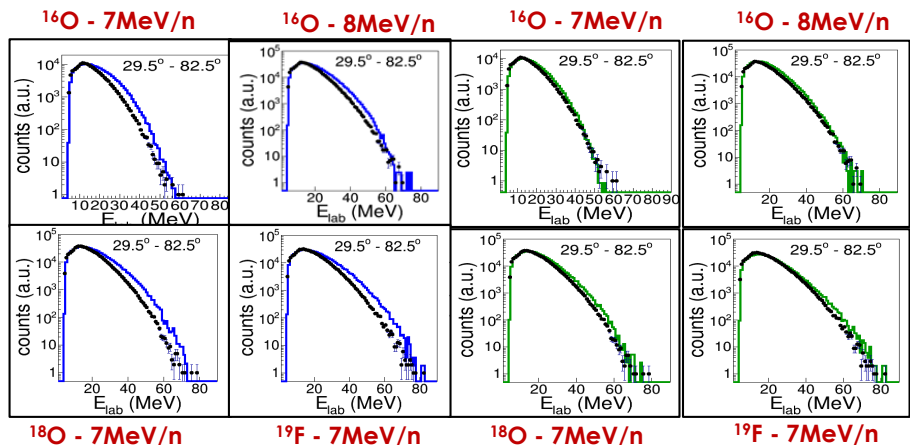
Reaction	E*(MeV)	η	ηE^*
$^{16}\text{O} + ^{30}\text{Si}$ 111 MeV	88	0,304	26,78
$^{16}\text{O} + ^{30}\text{Si}$ 128 MeV	98.4	0,304	29,95
$^{18}\text{O} + ^{28}\text{Si}$ 126 MeV	98.5	0,217	21,41
$^{19}\text{F} + ^{27}\text{Al}$ 133 MeV	103.5	0,174	18,00



Results: $Z_{\text{tot}} = Z_p + Z_t = 22$

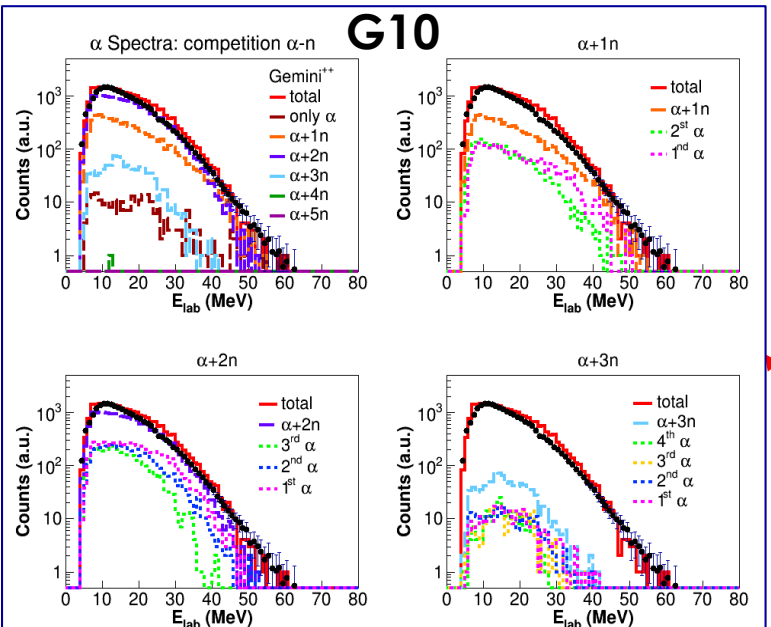
Decay channel competition – Energy spectra

G11 $Z_{\text{tot}}=22$ G00



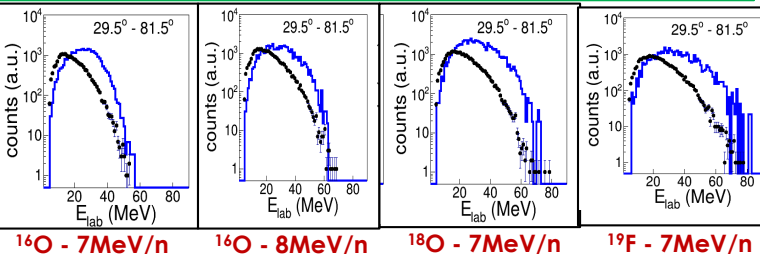
$^{16}\text{O} - 8\text{MeV/n}$

G10

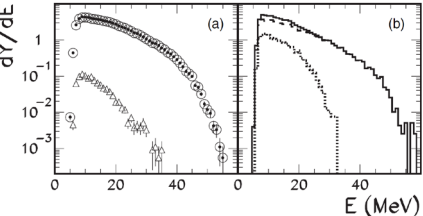


Different spectral shapes can derive from different decay chains contributions: either more n-emission or different priority in particle emission: This is even more evident in more exclusive channels

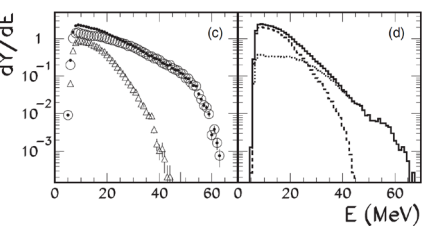
G11
 $Z_{\text{tot}}=22$
 $Z_{\text{ER}}=20$



From: L. Morelli et al. J. Phys. G: Nucl. Part. Phys. 41(2014)075107



AC
C+3 α decay channel vs C+2H +2 α decay channel: exp (left) vs HF/(right)

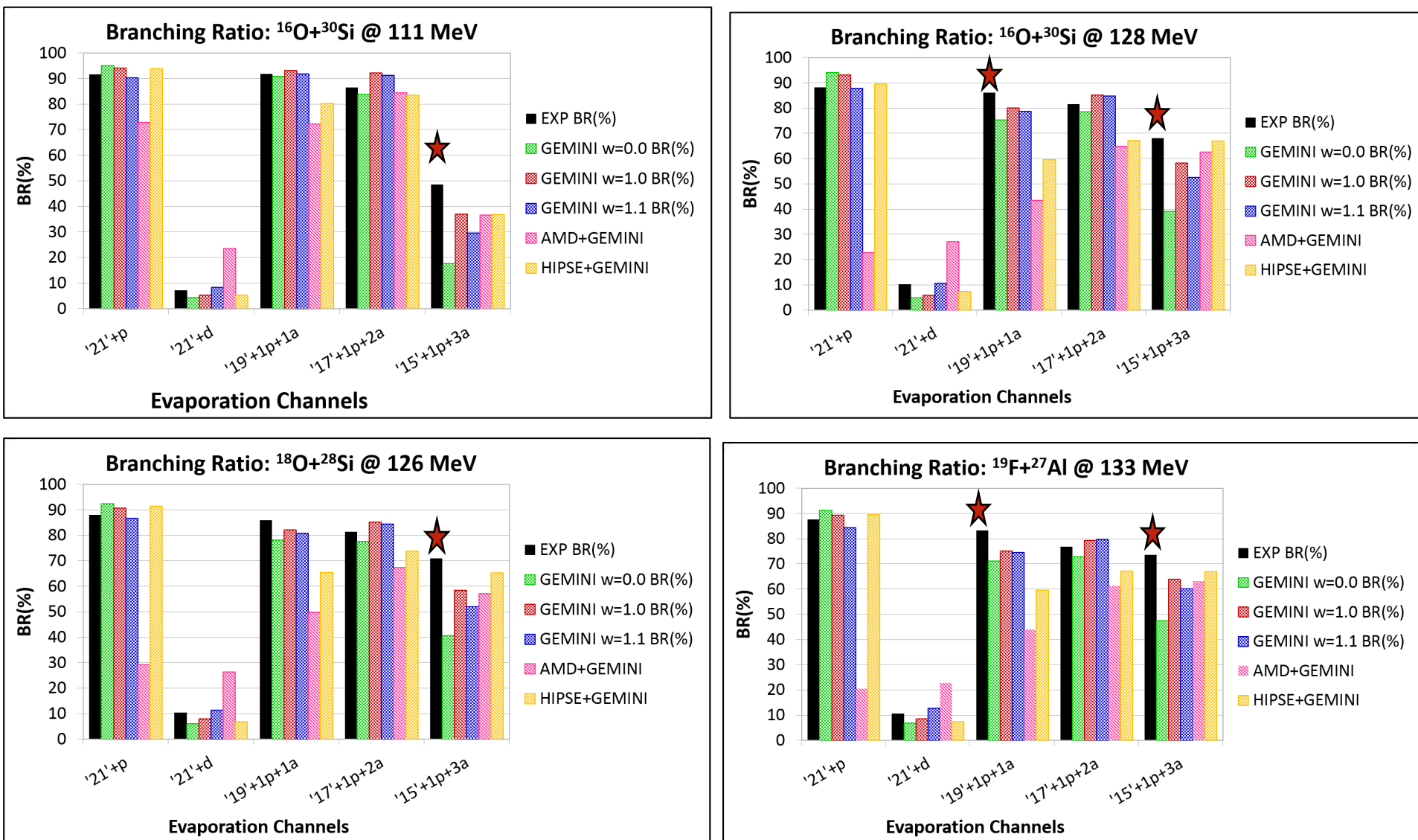


AO
O+2 α decay channel vs O+2 α +2H decay channel : exp (left) vs HF/(right)

Gemini⁺⁺: comparison to exp data from 4 π simulation including n-emission

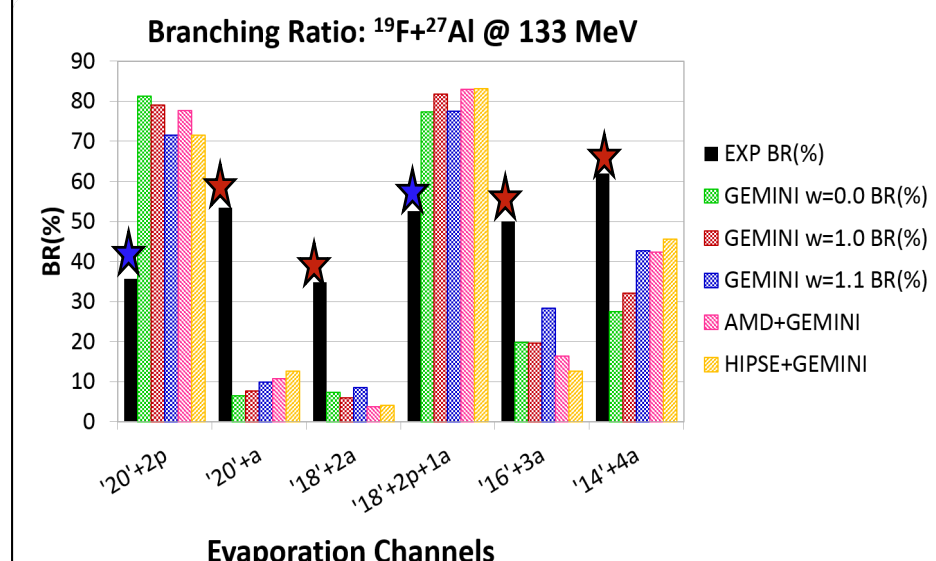
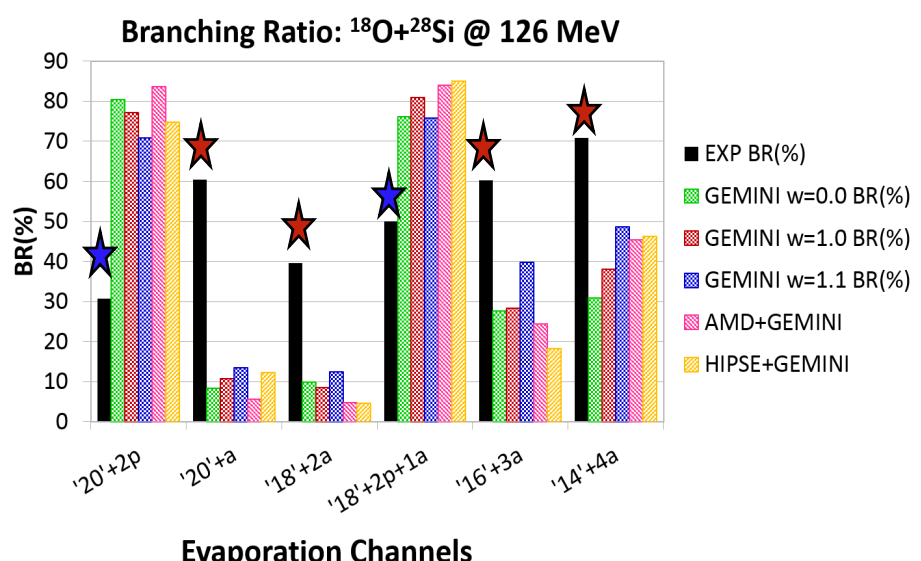
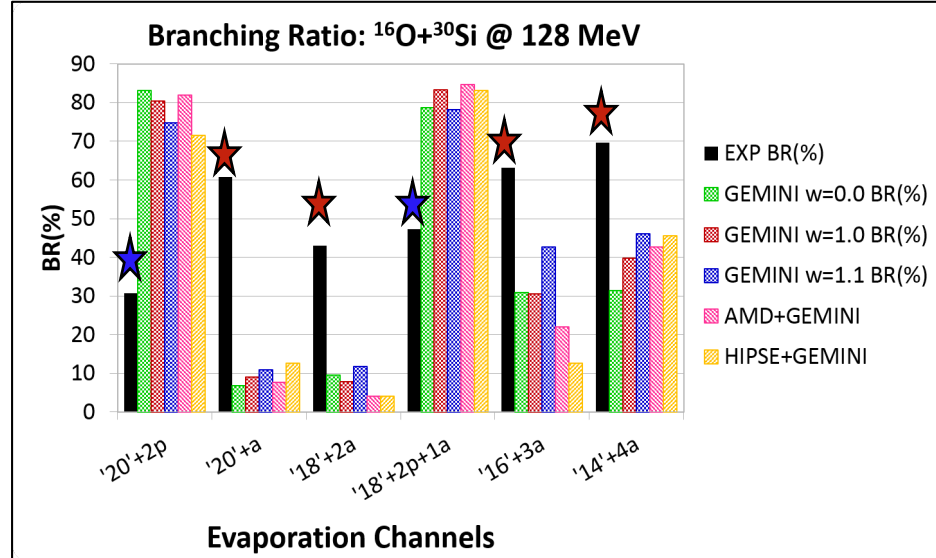
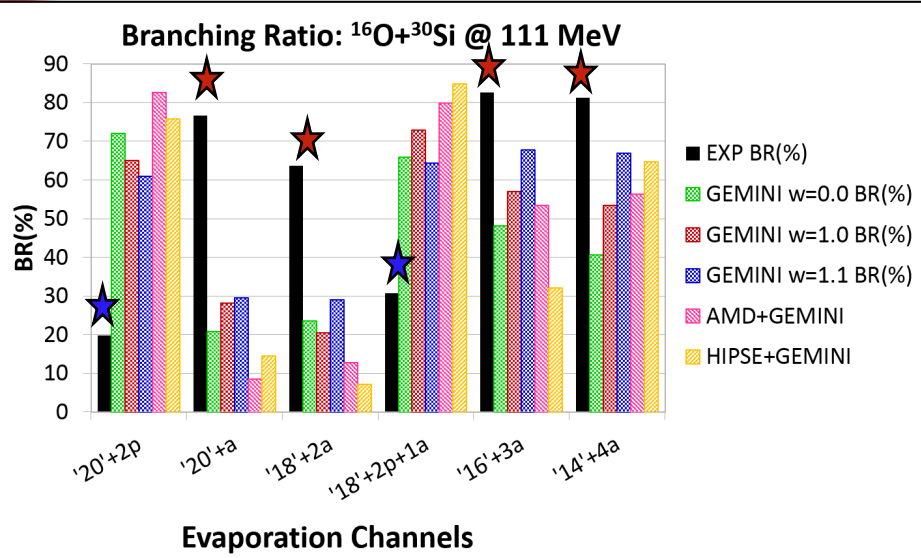
Results: $Z_{\text{tot}}=22$

Odd Z_{ER} - Branching Ratios



Results: $Z_{\text{tot}}=22$

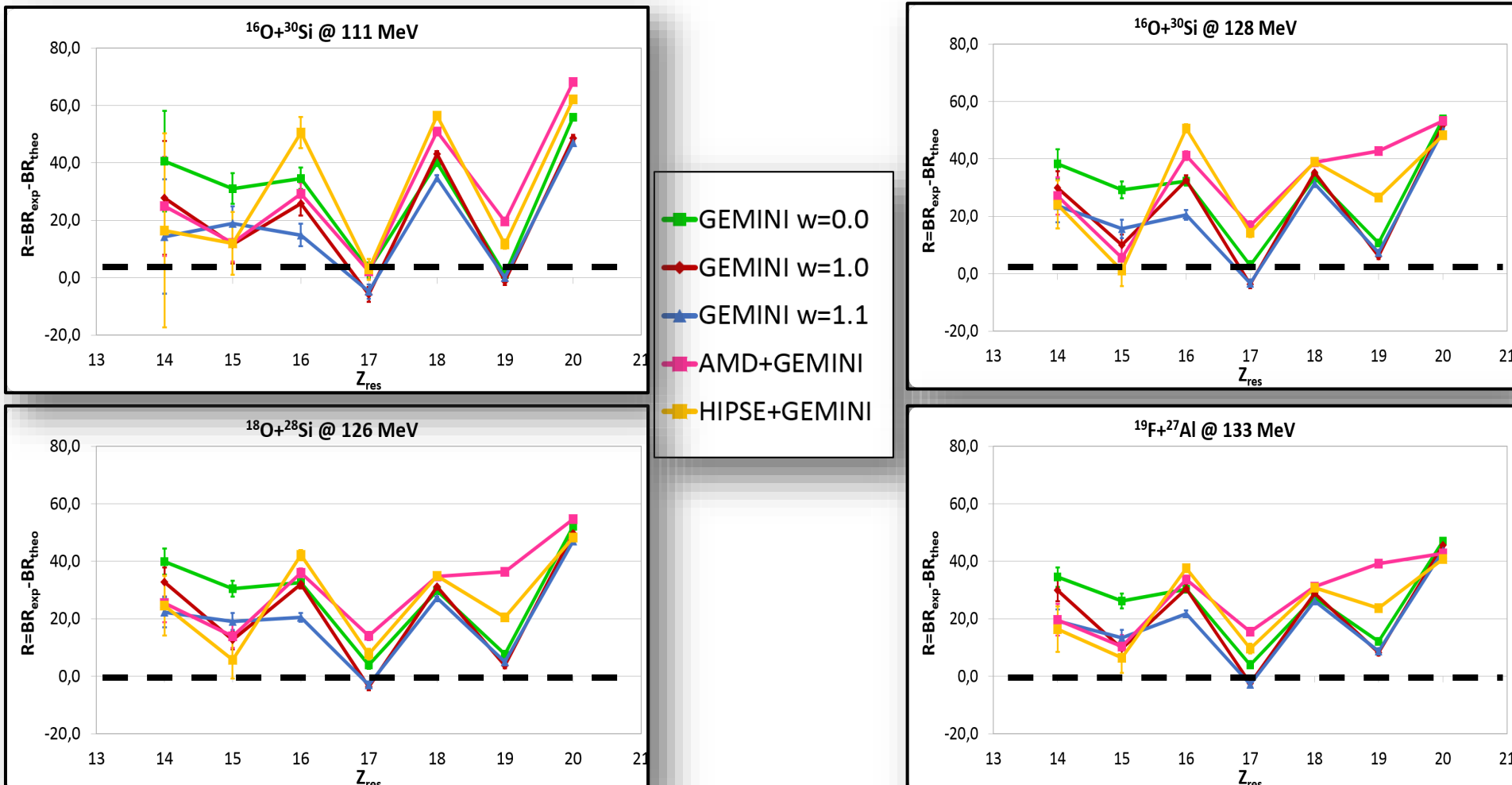
Even Z_{ER} - Branching Ratios



Results: $Z_{\text{tot}}=22$

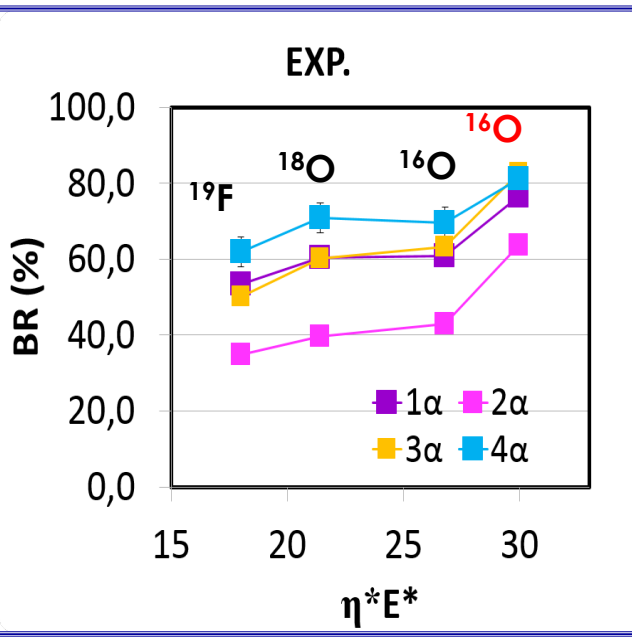
Branching Ratios: differences with Models

$$R = \frac{Y_{\text{exp}}(Z; n_z \alpha) - Y_{\text{theo}}(Z; n_z \alpha)}{Y_{\text{exp}}(Z)} - \frac{Y_{\text{theo}}(Z) - Y_{\text{theo}}(Z)}{Y_{\text{theo}}(Z)}$$

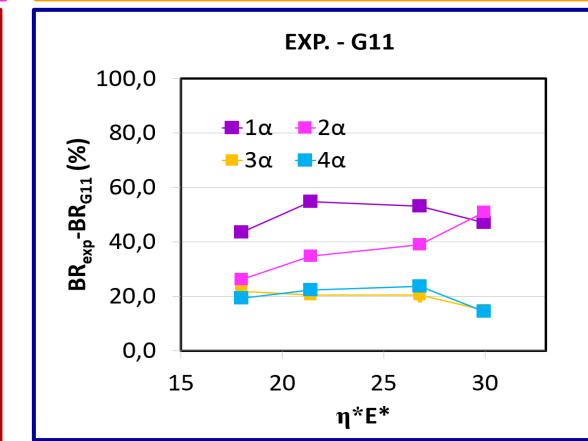
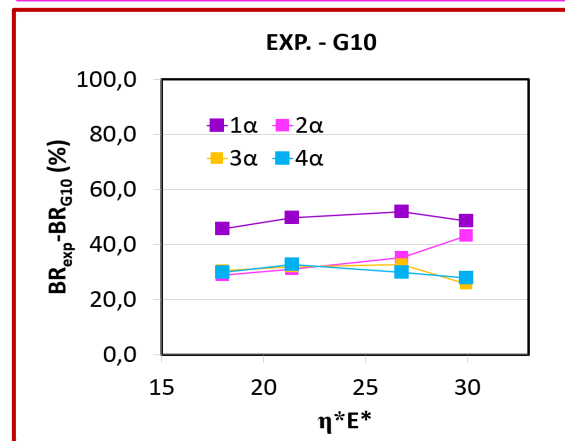
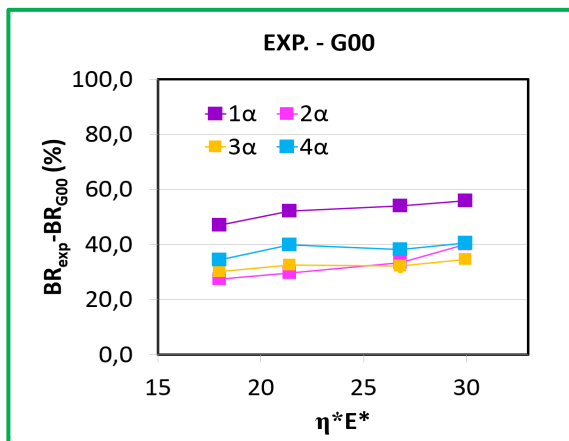
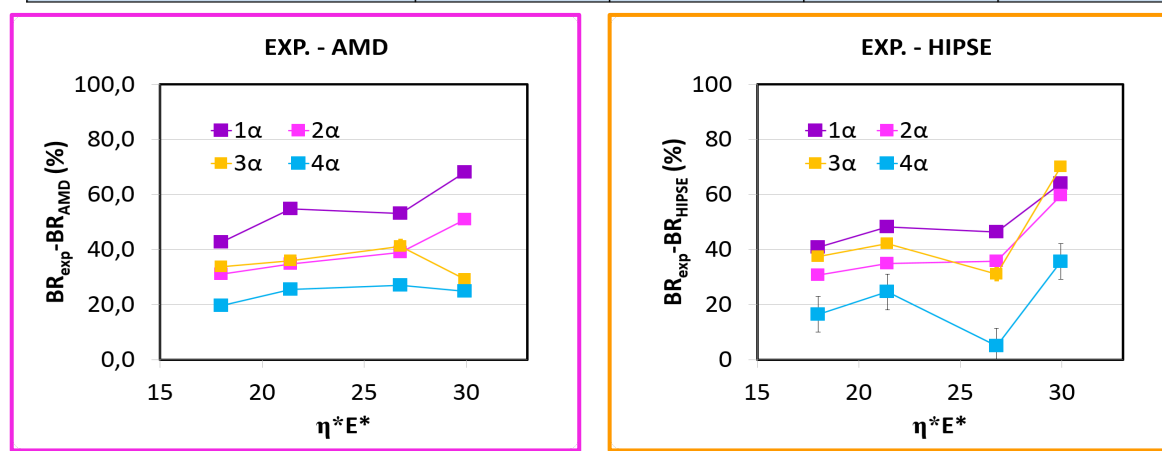


Results: $Z_{\text{tot}}=22$

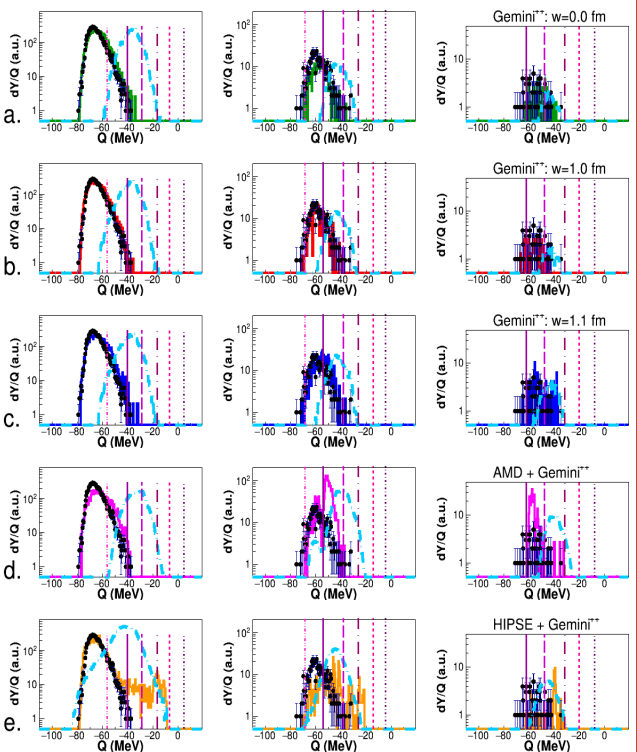
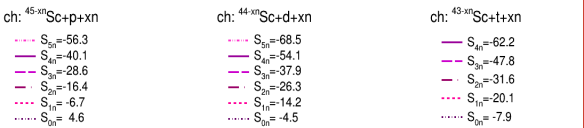
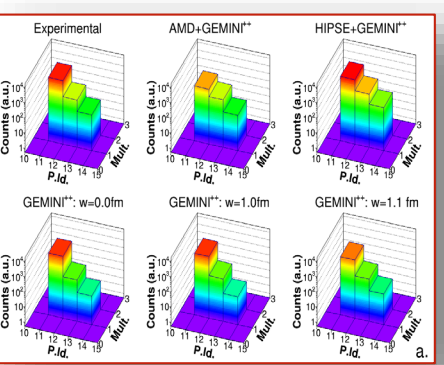
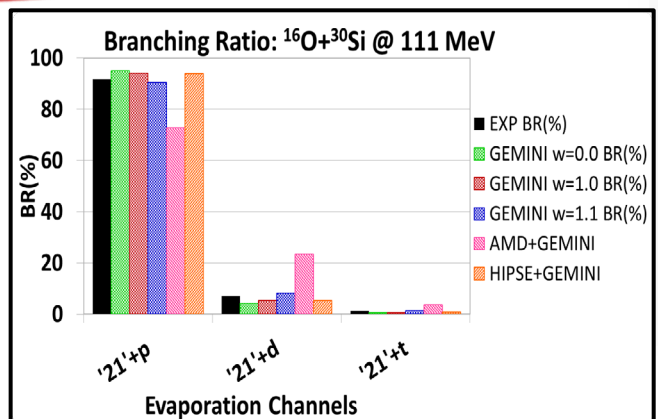
Branching Ratios



Reaction	η	E^*	η/E^*	$\eta \cdot E^*$
$^{16}\text{O}+^{30}\text{Si}@111\text{MeV}$	0,30	88	0,0035	26,78
$^{16}\text{O}+^{30}\text{Si}@128\text{MeV}$	0,30	98,4	0,0031	29,95
$^{18}\text{O}+^{28}\text{Si}@126\text{MeV}$	0,22	98,5	0,0022	21,41
$^{19}\text{F}+^{27}\text{Al}@133\text{MeV}$	0,17	103,5	0,0017	18,00



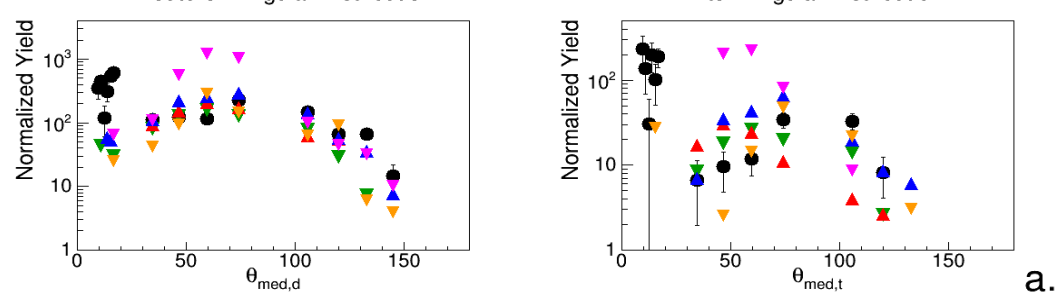
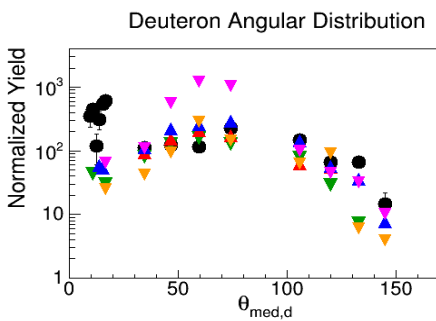
$Z_{\text{ER}}=21 - {}^{16}\text{O}+{}^{30}\text{Si}$ @ 111 MeV



${}^{16}\text{O}+{}^{30}\text{Si}$ @ 111 MeV

$Z_{\text{res}}=21$

- Exp.
- ▼ GEMINI⁺⁺: w=0.0fm
- ▲ GEMINI⁺⁺: w=1.0fm
- △ GEMINI⁺⁺: w=1.1fm
- AMD+GEMINI⁺⁺
- ◇ HIPSE+GEMINI⁺⁺

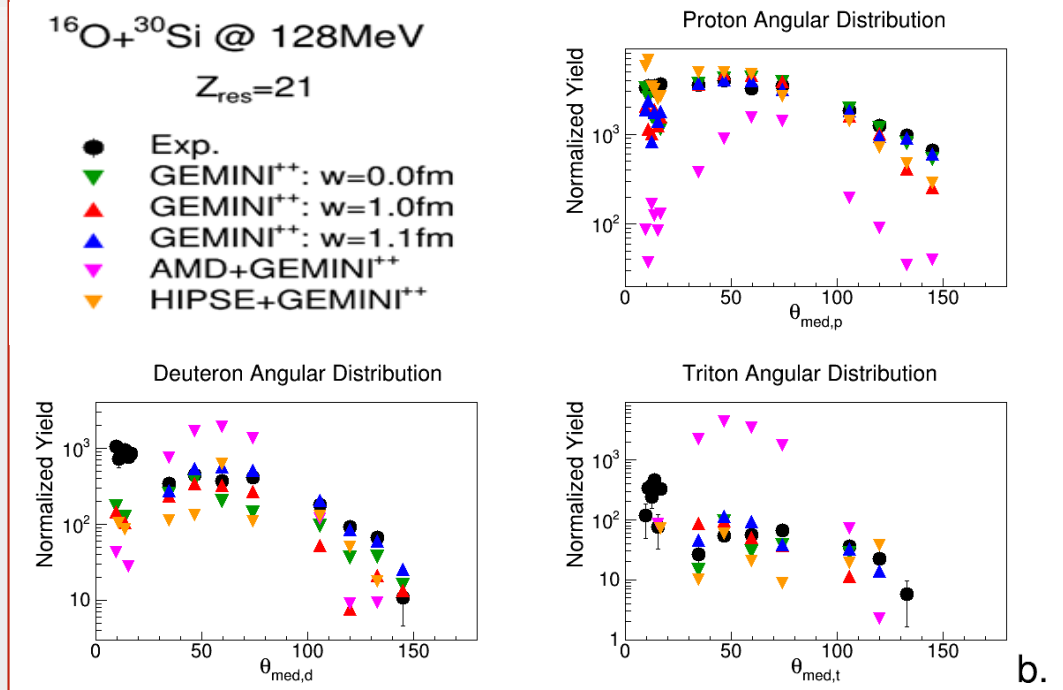
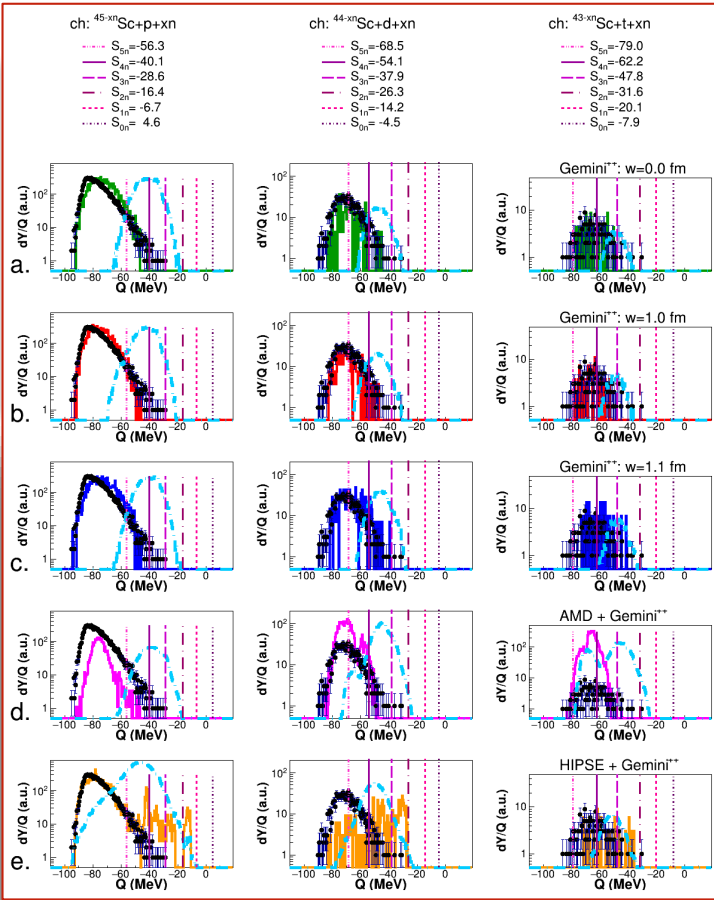
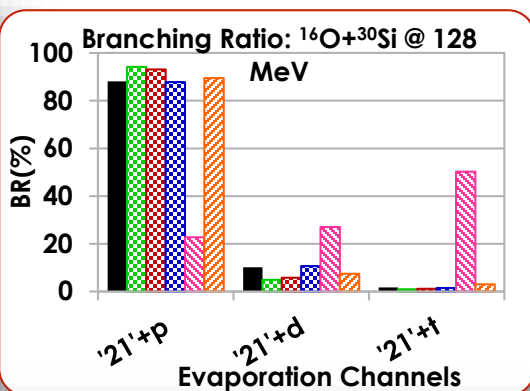
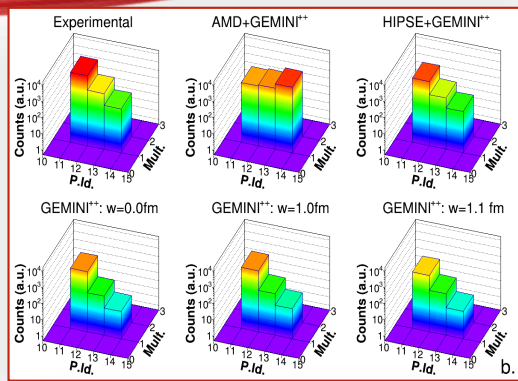


"Missing" Q-value

- ${}^{42}\text{Sc} + p + 3n$, followed by ${}^{43}\text{Sc} + p + 2n$ & ${}^{41}\text{Sc} + p + 4n$;
- ${}^{41}\text{Sc} + d + 3n$ followed by ${}^{42}\text{Sc} + d + 2n$;
- ${}^{41}\text{Sc} + t + 2n$.

Results: $Z_{\text{tot}}=22$

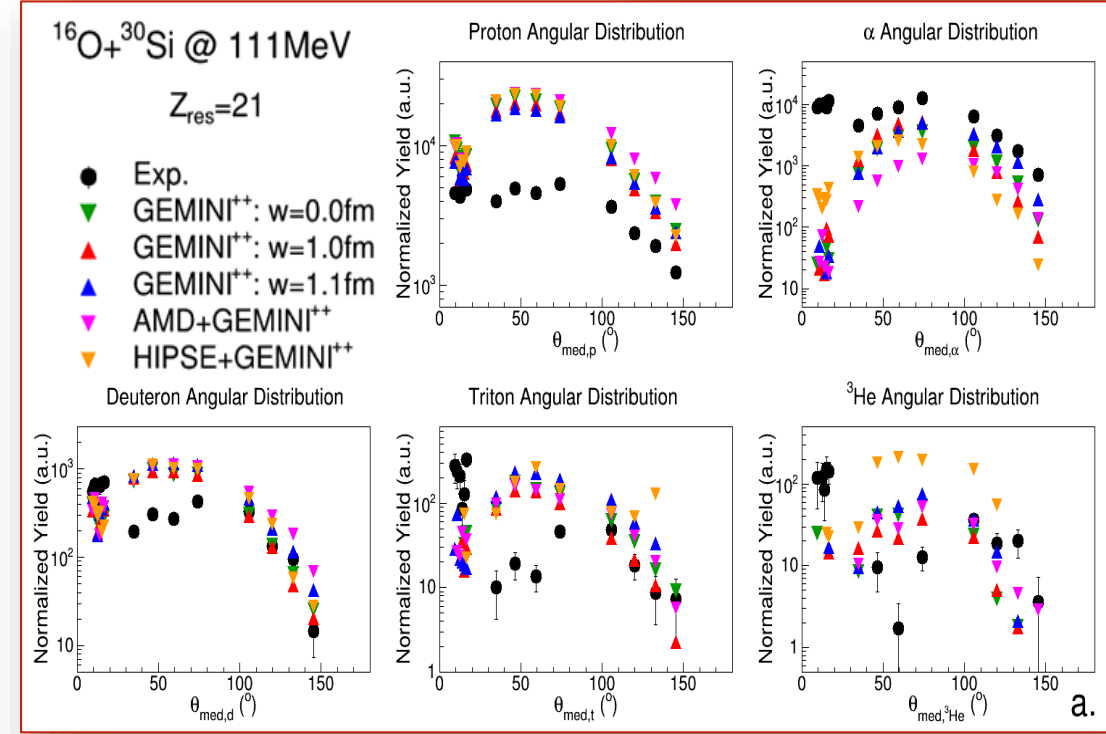
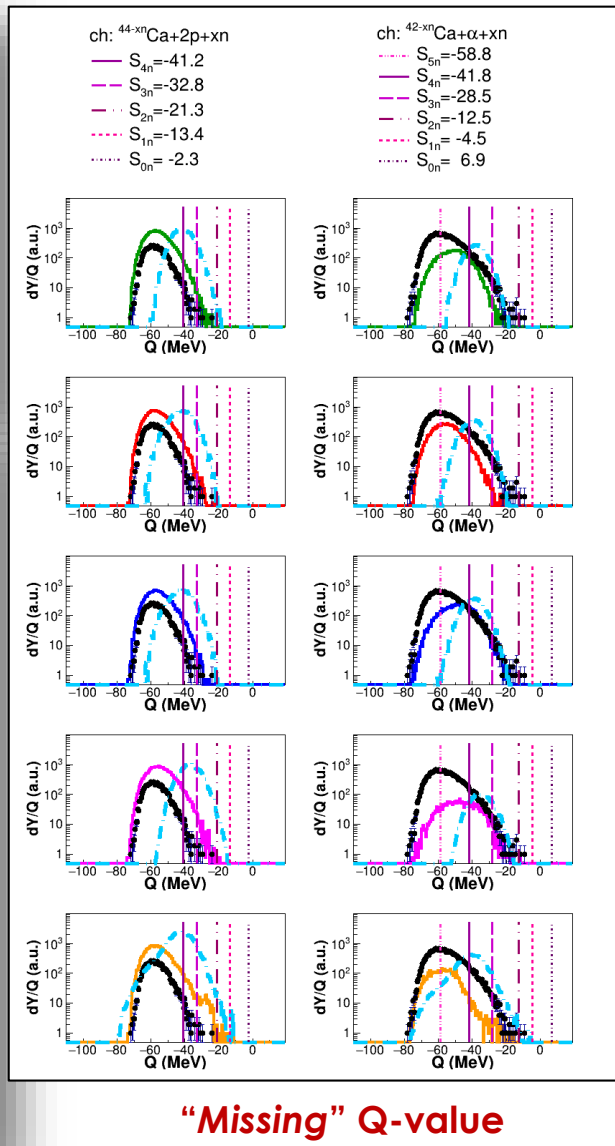
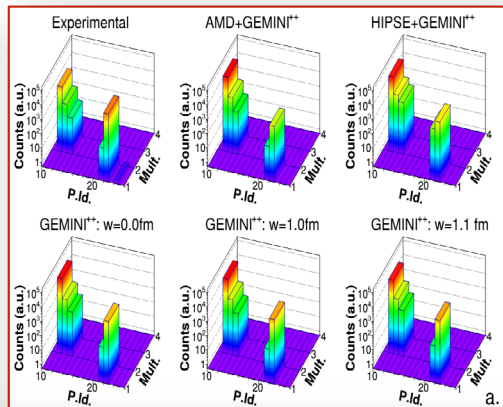
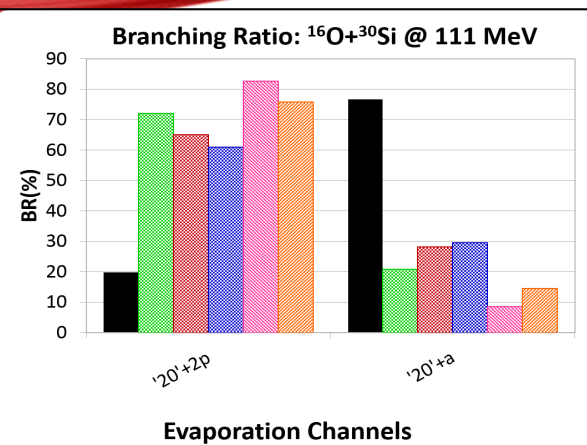
$Z_{\text{ER}}=21$ - $^{16}\text{O}+^{30}\text{Si}$ @ 128 MeV



- $^{42}\text{Sc} + \text{p} + 3\text{n}$ & $^{41}\text{Sc} + \text{p} + 4\text{n}$ followed by smaller yields $^{43}\text{Sc} + \text{p} + 2\text{n}$ & $^{41}\text{Sc} + \text{p} + 5\text{n}$;
- $^{41}\text{Sc} + \text{d} + 3\text{n}$ followed by $^{42}\text{Sc} + \text{d} + 2\text{n}$ & $^{40}\text{Sc} + \text{d} + 4\text{n}$;
- $^{41}\text{Sc} + \text{t} + 2\text{n}$ & $^{40}\text{Sc} + \text{t} + 3\text{n}$

Results: $Z_{\text{tot}}=22$

$Z_{\text{ER}}=20 - {}^{16}\text{O}+{}^{30}\text{Si}$ @ 111 MeV



"Missing" Q-value

G00

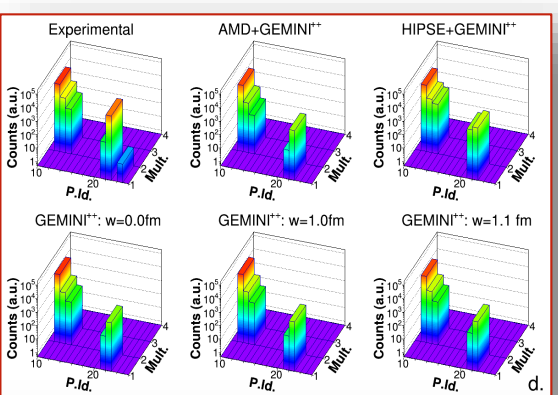
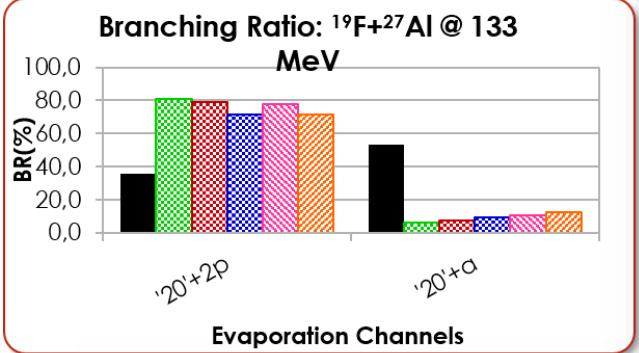
G10

G11

AMD

HIPSE

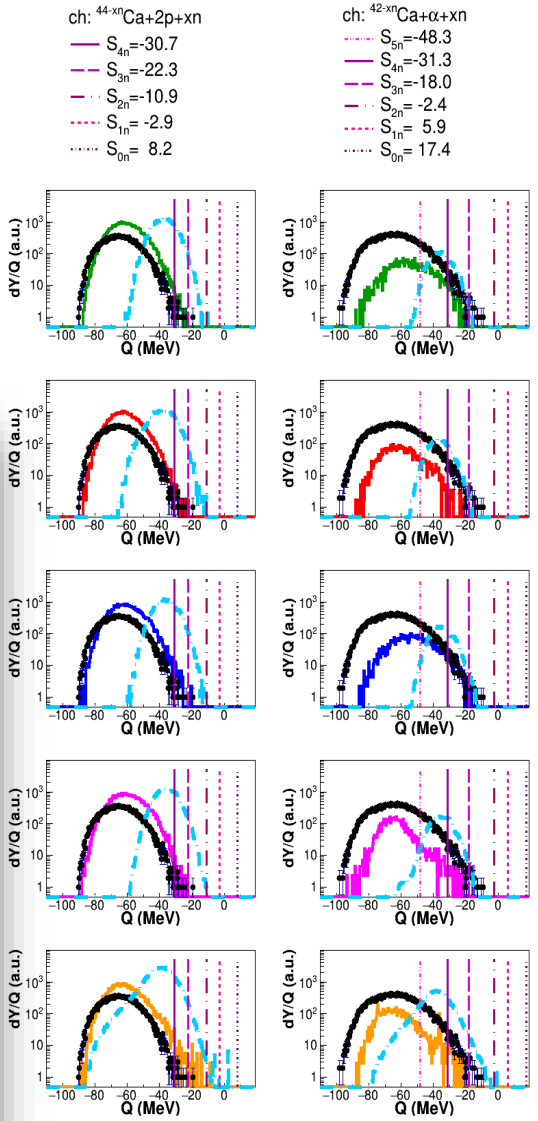
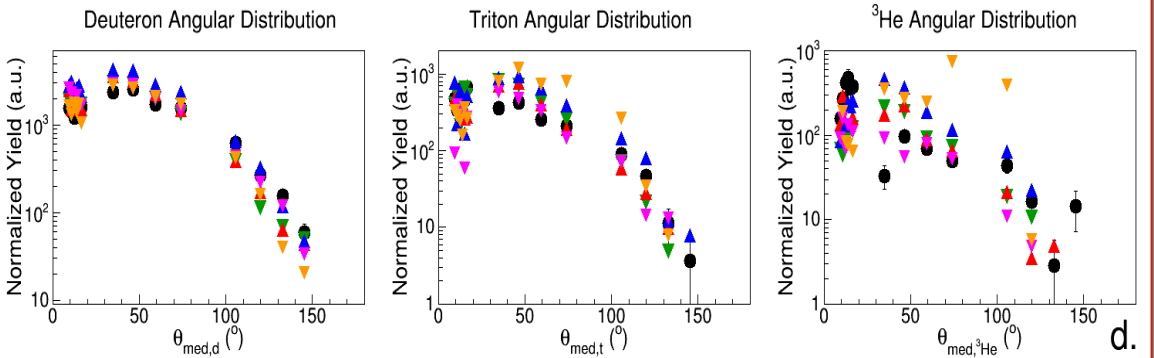
$Z_{\text{ER}}=20 - {}^{19}\text{F}+{}^{27}\text{Al}$ @ 133 MeV



ch: ${}^{44-xn}\text{Ca}+2p+xn$	$S_{4n}=-30.7$	$S_{5n}=-48.3$
	$S_{3n}=22.3$	$S_{4n}=-31.3$
	$S_{2n}=10.9$	$S_{3n}=-18.0$
	$S_{1n}=-2.9$	$S_{2n}=-2.4$
	$S_{0n}=8.2$	$S_{1n}=5.9$
		$S_{0n}=17.4$

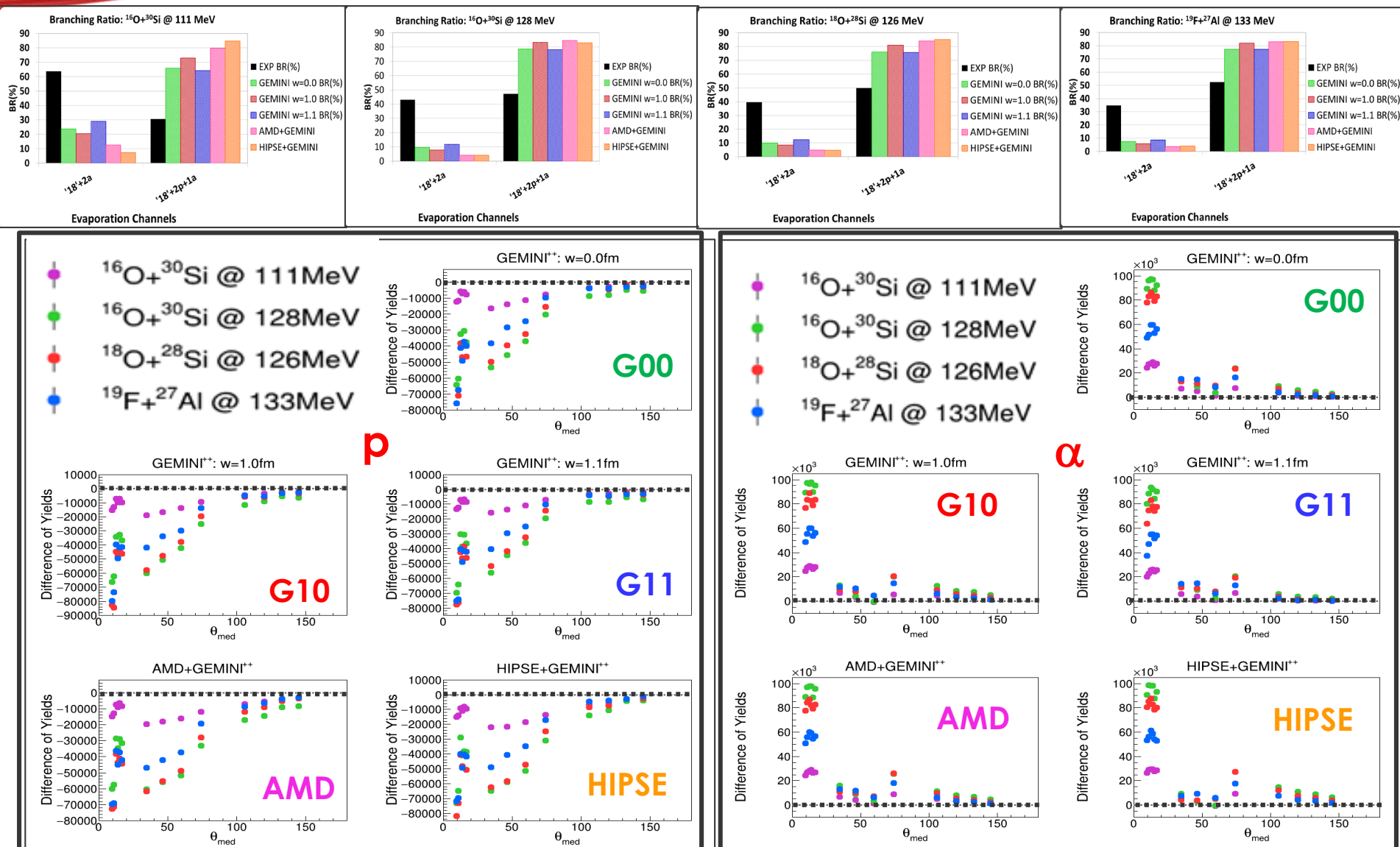
${}^{19}\text{F}+{}^{27}\text{Al}$ @ 133 MeV
 $Z_{\text{res}}=20$

- Exp.
- ▼ GEMINI⁺⁺: w=0.0fm
- ▲ GEMINI⁺⁺: w=1.0fm
- △ GEMINI⁺⁺: w=1.1fm
- AMD+GEMINI⁺⁺
- HIPSE+GEMINI⁺⁺



"Missing" Q-value

$Z_{\text{ER}} = 18$ – Difference in Ang. Distributions

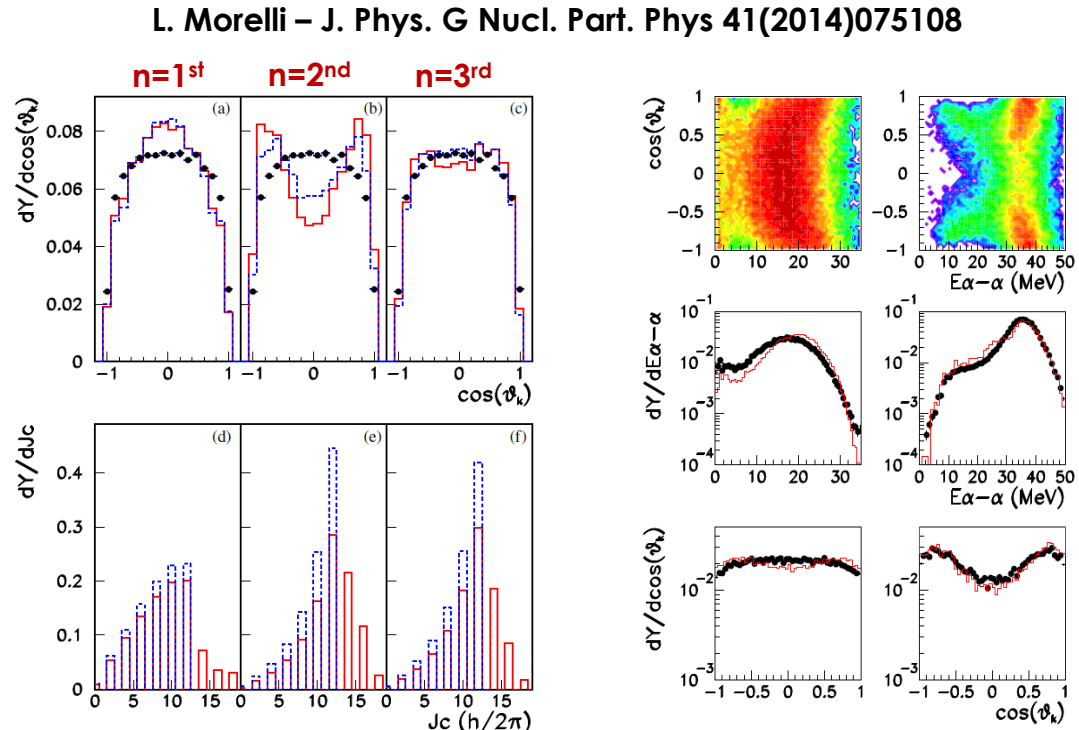


Results: $Z_{\text{tot}}=22$

$Z_{\text{ER}}=18 - 2\alpha$ correlations

$$E_{\alpha-\alpha} = \frac{\vec{k}_{\alpha-\alpha} \cdot \vec{k}_2}{2\mu}$$

$$\cos(\theta_k) = \frac{\vec{k}_{\text{residue}} \cdot \vec{k}_{\alpha-\alpha}}{|\vec{k}_{\text{residue}}| |\vec{k}_{\alpha-\alpha}|}$$



Shape of the $\cos(\theta_k)$ distribution: dependence on spin distribution involved in the process, which depends on **the priority of neutron emission in the cascade**.

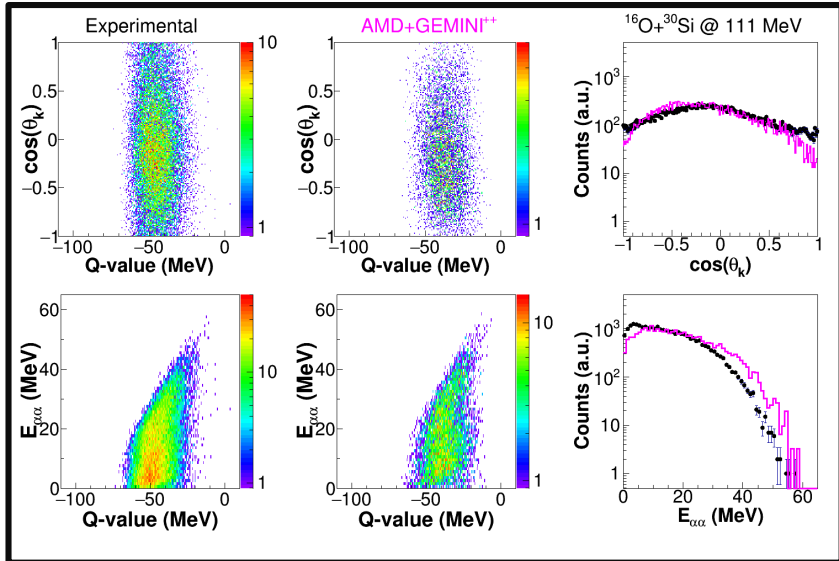
Example for the $^{12}\text{C} + ^{12}\text{C}$ at 95 MeV case.

Blue and red distributions are obtained by **Hauser Feshbach model** developed for light nuclei (**HF ℓ**) respectively with $J_{0\max}=18$ hbar ($\Delta J=2$) and $J_{0\max}=12$ hbar (sharp cut off).

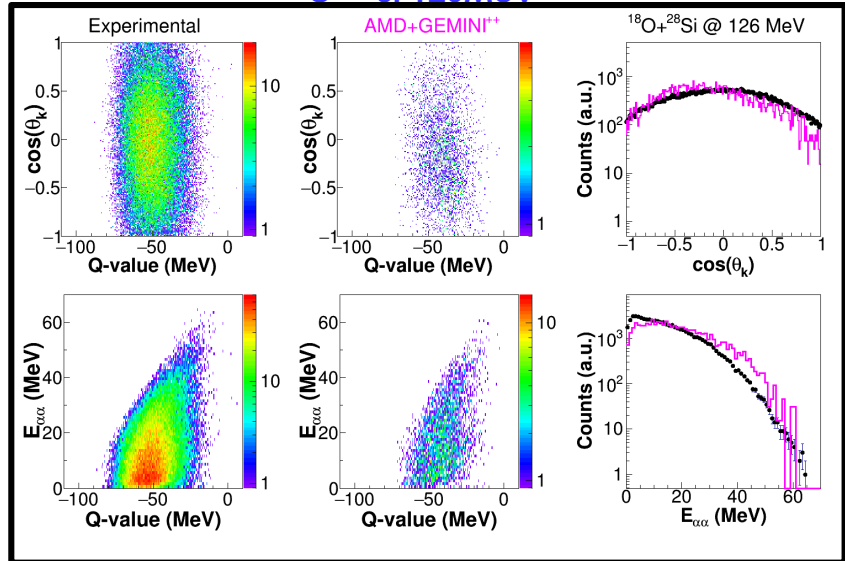
Results: $Z_{\text{tot}}=22$

$Z_{\text{ER}}=18 - 2\alpha$ correlations

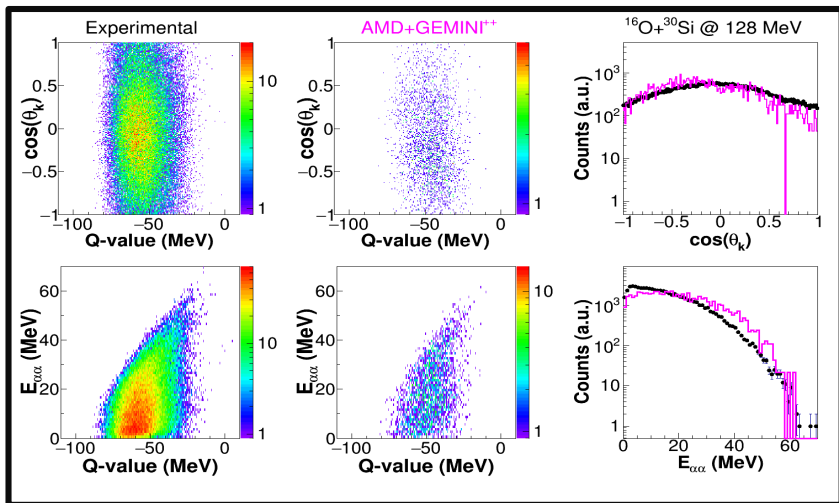
$^{16}\text{O}+^{30}\text{Si}$ 111 MeV



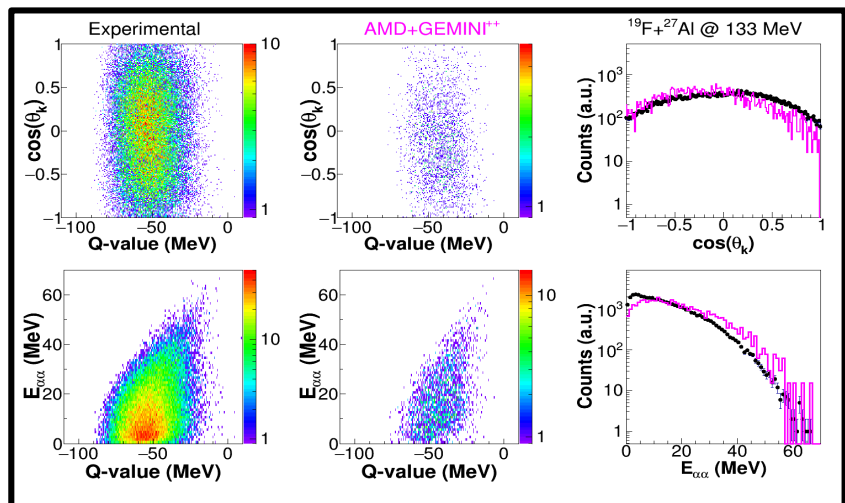
$^{18}\text{O}+^{28}\text{Si}$ 126 MeV



$^{16}\text{O}+^{30}\text{Si}$ 128 MeV



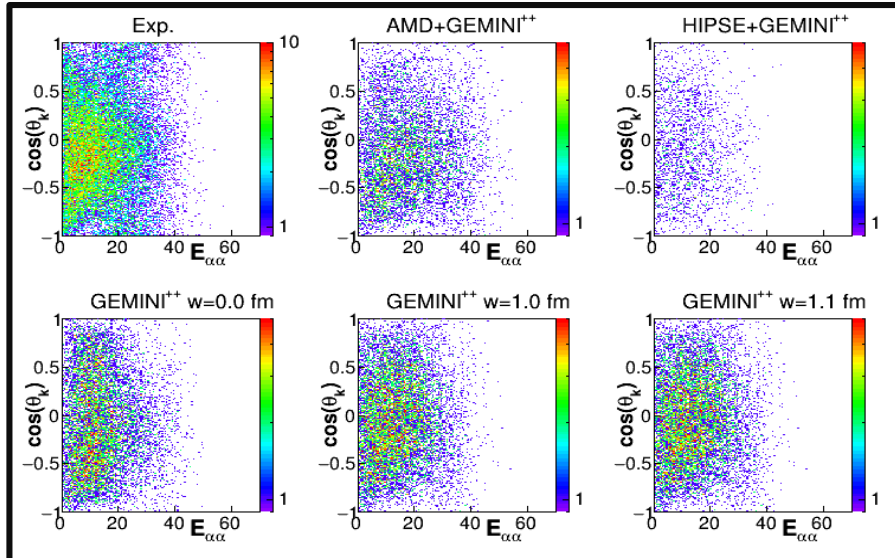
$^{19}\text{F}+^{27}\text{Al}$ 133 MeV



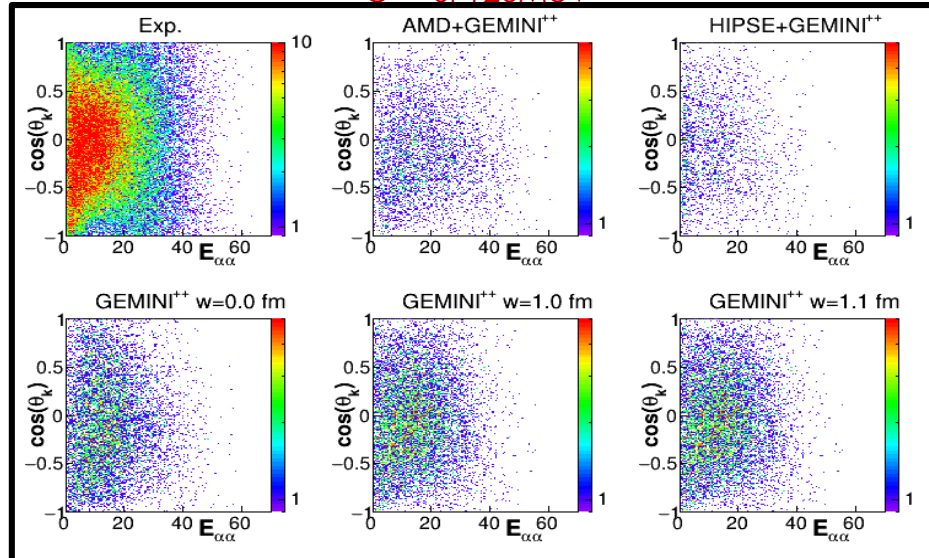
Results: $Z_{\text{tot}}=22$

$Z_{\text{ER}}=18 - 2\alpha$ correlations

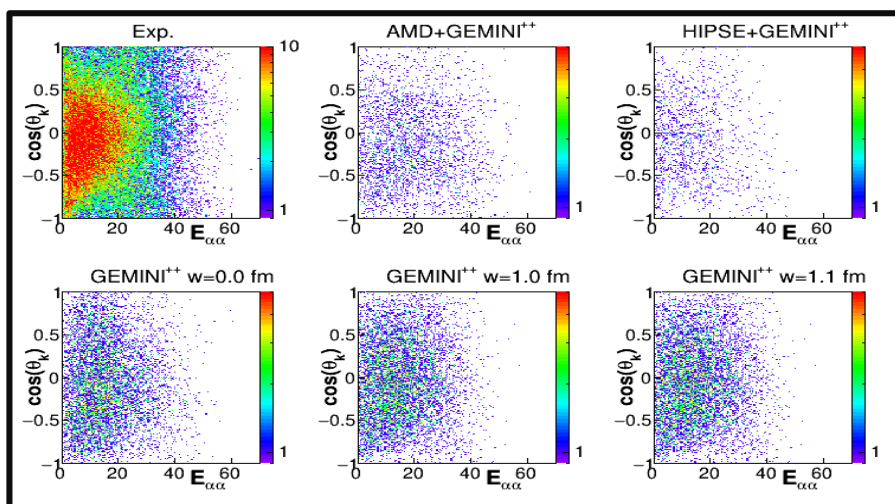
$^{16}\text{O}+^{30}\text{Si}$ 111 MeV



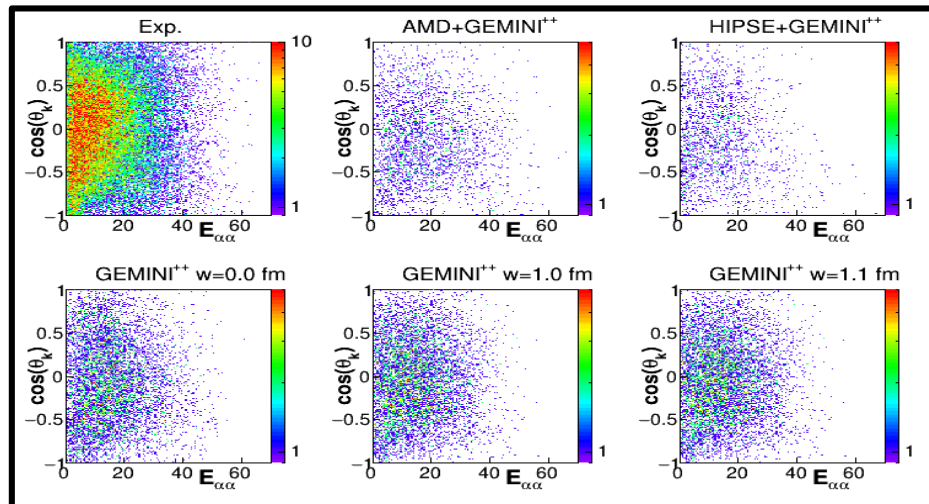
$^{18}\text{O}+^{28}\text{Si}$ 126 MeV



$^{16}\text{O}+^{30}\text{Si}$ 128 MeV

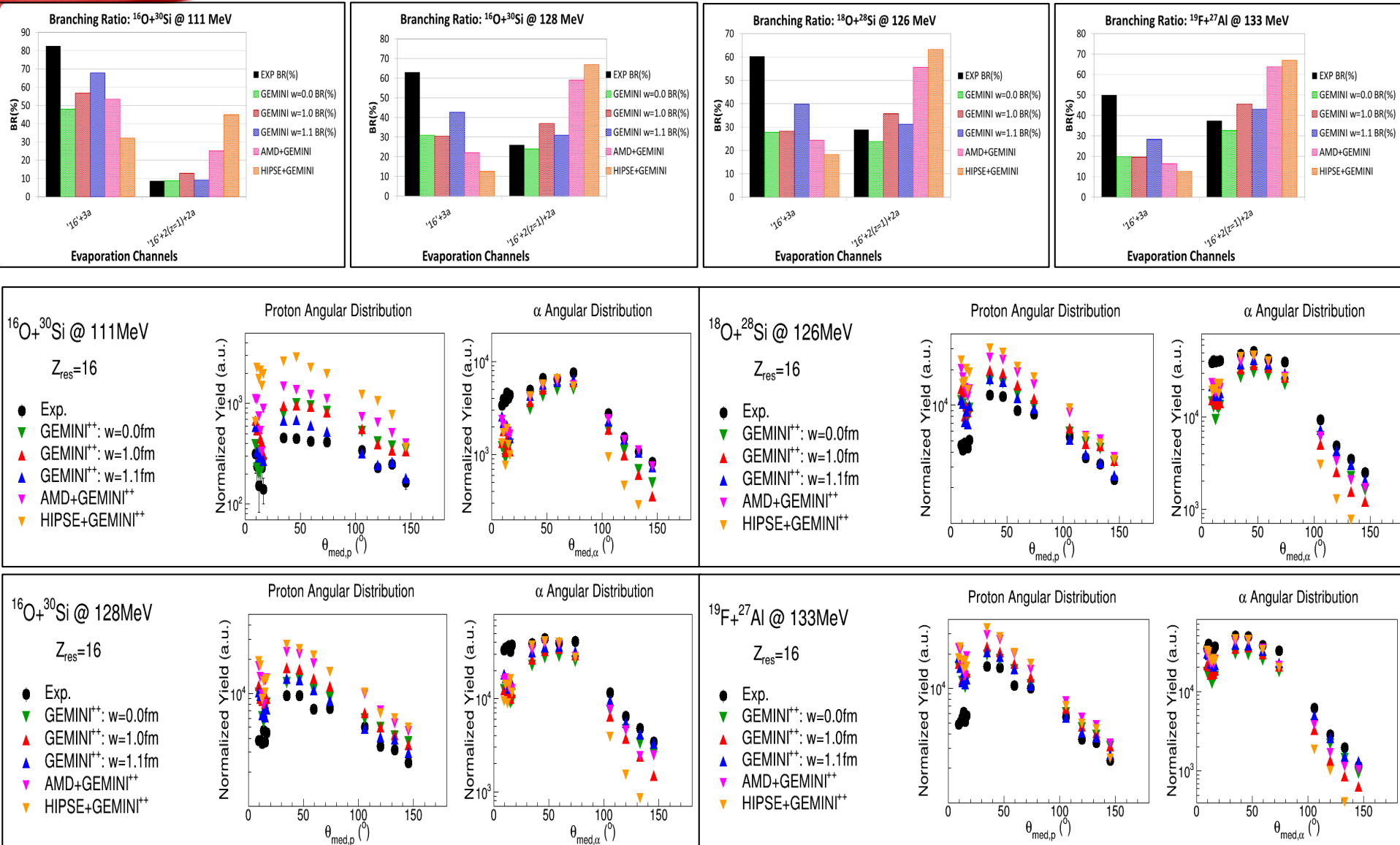


$^{19}\text{F}+^{27}\text{Al}$ 133 MeV



Results: $Z_{\text{tot}}=22$

$Z_{\text{ER}}=16 - 3\alpha$

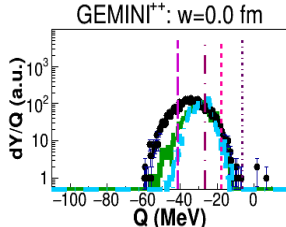


Results: $Z_{\text{tot}} = Z_p + Z_f = 22$

$Z_{\text{ER}} = 16 - Q\text{-values}$

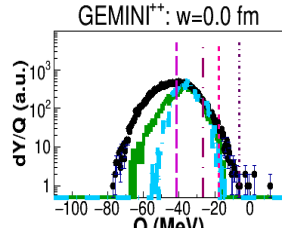
$^{16}\text{O} + ^{30}\text{Si}$ 111 MeV

a. ch: $^{34-xn}\text{S} + 3\alpha + xn$
 — S_{3n} = -41.6
 - S_{2n} = -26.6
 - S_{1n} = -17.9
 - S_{0n} = -6.5



$^{16}\text{O} + ^{30}\text{Si}$ 128 MeV

a. ch: $^{34-xn}\text{S} + 3\alpha + xn$
 — S_{3n} = -41.6
 - S_{2n} = -26.6
 - S_{1n} = -17.9
 - S_{0n} = -6.5

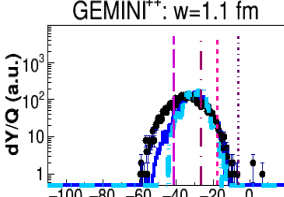
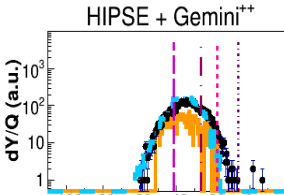


AMD + Gemini⁺⁺

HIPSE + Gemini⁺⁺

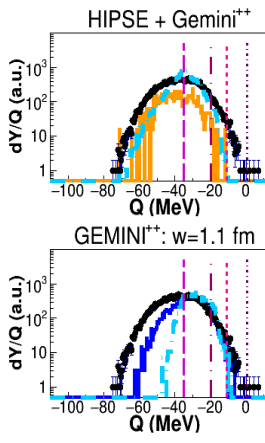
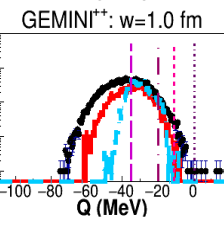
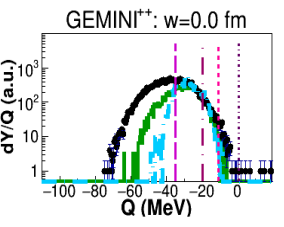
GEMINI⁺⁺: $w=1.0$ fm

GEMINI⁺⁺: $w=1.1$ fm



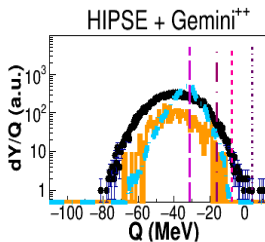
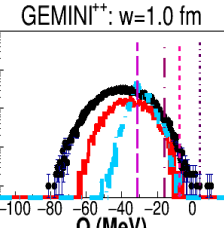
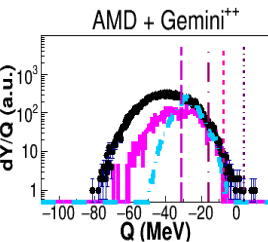
$^{18}\text{O} + ^{28}\text{Si}$ 126 MeV

a. ch: $^{34-xn}\text{S} + 3\alpha + xn$
 — S_{3n} = -34.9
 - S_{2n} = -19.7
 - S_{1n} = -11.0
 - S_{0n} = 0.4



$^{19}\text{F} + ^{27}\text{Al}$ 133 MeV

a. ch: $^{34-xn}\text{S} + 3\alpha + xn$
 — S_{3n} = -31.1
 - S_{2n} = -16.1
 - S_{1n} = -7.4
 - S_{0n} = 4.0



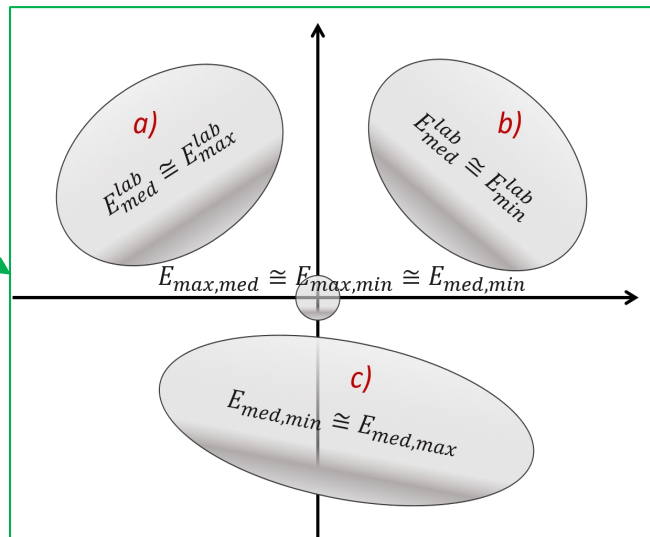
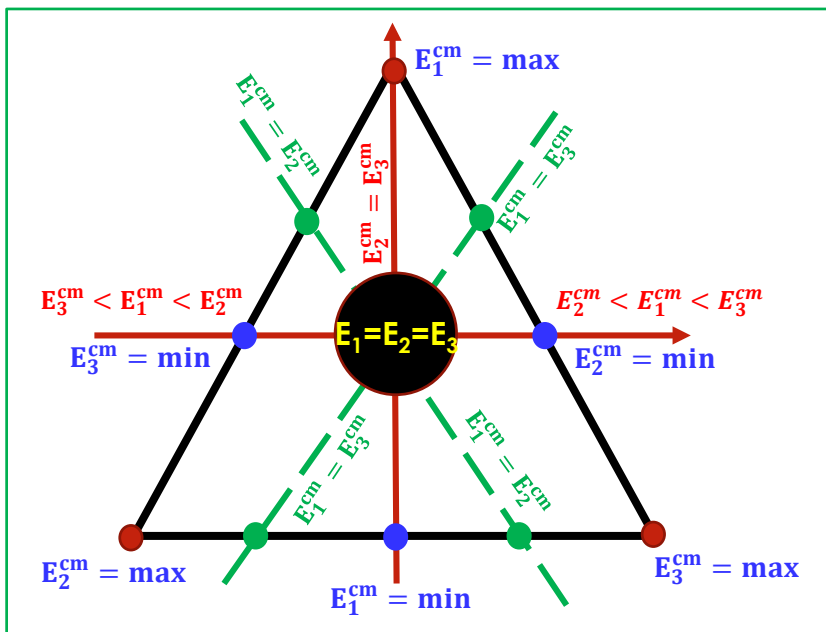
Results: $Z_{\text{tot}}=22$

$Z_{\text{ER}}=16 - 3\alpha$ DALITZ PLOTS

DALITZ 1: relative energies

$$x_D = \sqrt{3} \frac{E_{\max,med} - E_{med,min}}{2}$$

$$y_D = \frac{2E_{\max,min} - E_{\max,med} - E_{med,min}}{2}$$



DALITZ 2: absolute cm energies

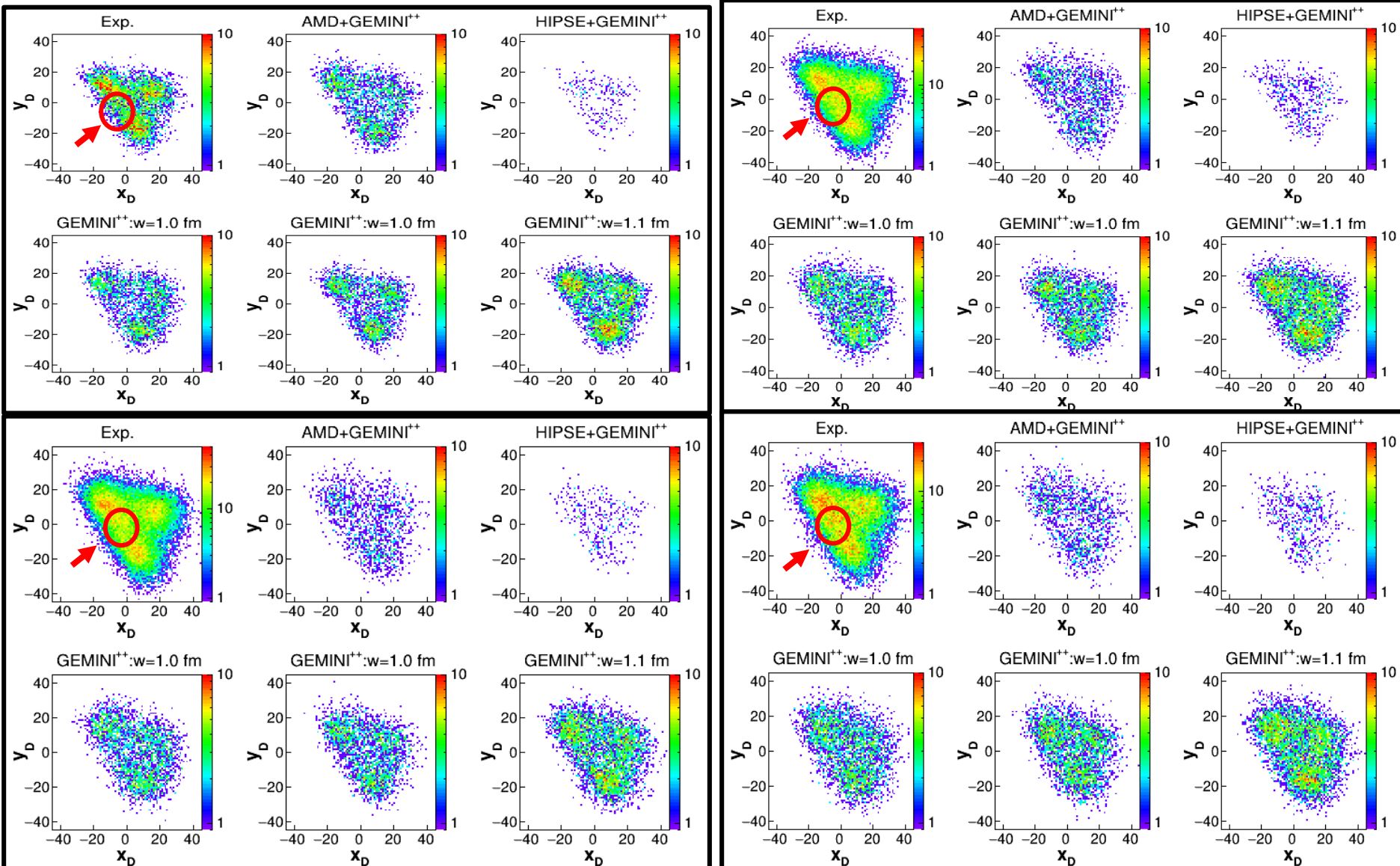
Starting from ordered E^{lab} : $E_1^{\text{lab}} < E_2^{\text{lab}} < E_3^{\text{lab}}$

$$x_D = \sqrt{3} \frac{E_3^{\text{cm}} - E_2^{\text{cm}}}{2}$$

$$y_D = \frac{2E_1^{\text{cm}} - E_3^{\text{cm}} - E_2^{\text{cm}}}{2}$$

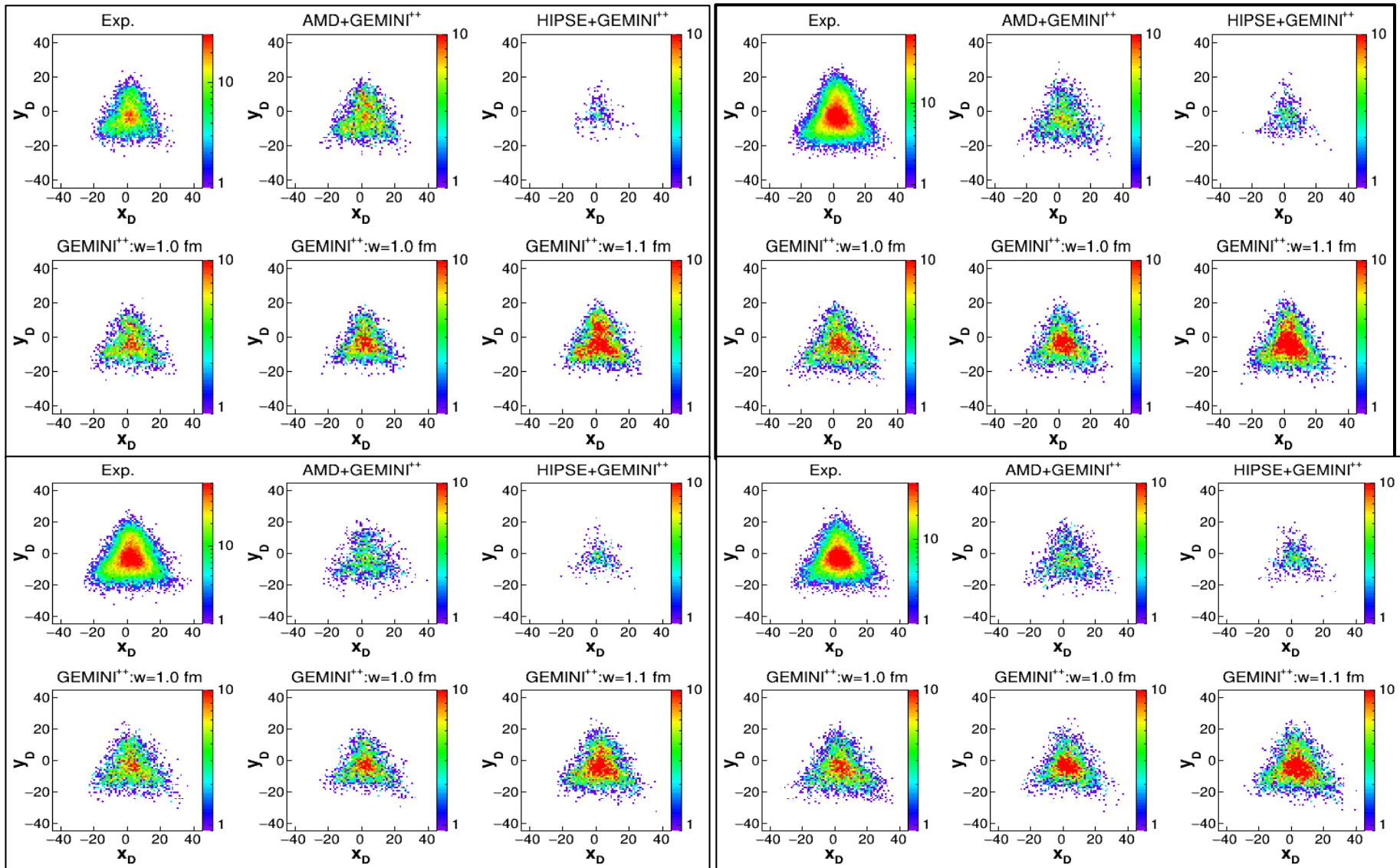
Results: $Z_{\text{tot}}=22$

Dalitz Plots $1 \rightarrow Z_{\text{ER}}=16 \& 3\alpha$



Results: $Z_{\text{tot}}=22$

Dalitz Plots $2 \rightarrow Z_{\text{ER}}=16 \text{ & } 3\alpha$



- Observing the **decay** of $^{46}\text{Ti}^*$, through the **quasi-complete events ($Z_{\text{tot}} > 18$)** → a reasonable **reproduction** by model predictions of the **major part of global variables**
- nevertheless, **some differences** observed → crucial in the study of the **interplay** between the **two different reaction mechanisms**: **α -particles overproduction** observed at **forward angles**, which represents a **signature of the onset of fast emission** not reproduced by dynamical models.
- Looking in more details **complete events ($Z_{\text{tot}} = 22$)**:
 - **BR** for **odd Z residues** are **well reproduced** – observed **differences in ang distrib. & energy spectra**
 - **BR** for **even Z residues** are quite **different** from **model predictions**:
 - ✓ **overproduction** of **multiple- α channels**, in which **pure α -particles (plus n)** are emitted.
 - ✓ **forward emission component** evident at variance with **p** which are correspondingly **depleted**.
 - **particle-particle correlations, selecting specific decay channels (1 α , 2 α 3 α .. channels)** show some peculiarities in the experimental data:
 - ✓ especially at higher E^* **larger exp dissipations** (**more n-evaporation expected**) in the **α -decay channels**;
 - ✓ Exp. peak at small relative energy correlations (**^{8}Be decay?**) in the **2 α** channel
 - ✓ **equal energy** and **equal relative energy** of the **3 α** → not accounted for by models both as **yields and shapes**.
 - Observed **experimental trends** vs. ηE^* of **different variables** → not reproduced by models → **possible extra (structure?) effects** in the dynamics of the reaction.

... and Perspectives

- Final consideration on obtained results are still **under discussion** due to the huge amount of data and findings → Dynamical models/phase to be better described → **discussion/collaboration ongoing**.
- Further **AMD simulations** are in progress with **different parameter sets (σ_{NN} – clustering etc.)**.

**M. Cicerchia –
PhD work @UNIPD**



COLLABORATION

M.Cicerchia^{1,2}, **F. Gramegna¹**, D. Fabris³, T. Marchi¹, M. Cinausero¹, G. Mantovani^{1,2}, A. Caciolli^{2,3}, G. Collazuol^{2,3}, D. Mengoni^{2,3}, M. Degerlier⁴, L. Morelli⁵, M. Bruno⁵, M. D'Agostino⁵, S. Barlini⁶, S. Piantelli⁶, M. Bini⁶, G. Pasquali⁶, P. Ottanelli⁶, G. Casini⁶, G. Pastore⁶, C. Frosin⁶, D. Gruyer⁷, A. Camaiani⁶, S. Valdré⁶, N. Gelli⁶, A. Olmi⁶, G. Poggi⁶, I. Lombardo⁸, D. Dell'Aquila^{8,9}, S. Leoni¹⁰, N. Cieplicka-Orynczak¹⁰⁻¹¹, B. Fornal¹¹, V.L. Kravchuk¹², J. Mabiala¹³.

¹INFN Laboratori Nazionali di Legnaro, Legnaro (PD), Italy.

²Dipartimento di Fisica e Astronomia dell'Università di Padova, Padova, Italy.

³INFN Sezione di Padova, Padova, Italy.

⁴Science and Art Faculty, Physics Department, Nevsehir Haci Bektaş Veli Univ., Nevsehir, Turkey.

⁵INFN Sezione di Bologna e Dipartimento di Fisica e Astronomia, Univ. di Bologna, Bologna, Italia.

⁶INFN Sezione di Firenze e Dipartimento di Fisica e Astronomia, Univ. di Firenze, Firenze, Italia.

⁷Grand Accélérateur National d'Ions Lourds, 14076 Caen, France,

⁸INFN Sezione di Catania, Catania, Italia.

⁹Institut de Physique Nucléaire (IPN) Université Paris-Sud 11, Orsay, Île-de-France, France.

¹⁰INFN Sezione di Milano e Dipartimento di Fisica, Univ. di Milano, Milano, Italia.

¹¹Institute of Nuclear Physics, Polish Academy of Sciences Krakow, Poland.

12 National Research Center - Kurchatov Institute- Moscow, Russia

13 Prairie View A&M University, Houston, TX, USA

Akira Ono - Department of Physics, Tohoku University, Sendai 980-77, (Japan) → AMD

Davide Mancusi - CEA-Saclay (France) → GEMINI++

Denis Lacroix - IPN Orsay (France) → HIPSE

THANK YOU

